RECLAMATION

Managing Water in the West

Technical Memorandum TM-85-833000-2014-45

Considerations in Raising the Maximum Allowable Surface Injection Pressure (MASIP) at Paradox Valley

Colorado Basin Salinity Control Project,
Paradox Valley Unit, Colorado
Upper Colorado Region

U.S. Department of the Interior
Bureau of Reclamation

November 2015

Mission Statements

The mission of the Department of the Interior is to protect and provide access to our Nation's natural and cultural heritage and honor our trust responsibilities to Indian Tribes and our commitments to island communities.

The mission of the Bureau of Reclamation is to manage, develop, and protect water and related resources in an environmentally and economically sound manner in the interest of the American public.

BUREAU OF RECLAMATION
Technical Service Center, Denver, Colorado
Seismology, Geomorphology, and Geophysics Group, 85-833000

Technical Memorandum TM-85-833000-2014-45

Considerations in Raising the Maximum Allowable Surface Injection Pressure (MASIP) at Paradox Valley

Colorado Basin Salinity Control Project,
Paradox Valley Unit, Colorado
Upper Colorado Region

Prepared by:

William Yeck, Geophysicist — 5/15/15 Date

Lisa Block, Geophysicist — 11/23/15 Date

Peer Review Certification

This report has been reviewed and is believed to be in accordance with the service agreement and standards of the profession.

Peer reviewed by:

Christopher Wood, Geophysicist — 11/23/15 Date

Contents

Tables

Figures

Page

1 Introduction

The Bureau of Reclamation (Reclamation) operates a deep injection well at Paradox Valley in western Colorado (Figure 1) as part of the Paradox Valley Unit (PVU) of the Colorado River Basin Salinity Control Program (CRBSCP). The Colorado River Basin Salinity Control Act of 1974 authorized the PVU for construction (Public Law 93-320; amended in 1984 as Public Law 98-569). The objective of the PVU is to reduce the salt load of the Colorado River. The Dolores River, a tributary of the Colorado River, picks up nearly 185,000 metric tons of salt annually from natural brine groundwater inflow in the Paradox Valley. Because Paradox Valley overlies a salt anticline, groundwater in the valley has a salt concentration nearly eight times that of ocean water. Currently, the PVU diverts up to 90 percent of Paradox Valley brine inflow from entering the Dolores River. Subsurface brine flow is intercepted by the pumping of shallow extraction wells located along the river (Figure 2). The extracted brine is collected and filtered at a surface treatment facility, piped 3.6 miles (6 km) to a facility at the edge of the valley, and injected into a 15,900-ft (4.8-km) deep injection well (PVU Injection Well #1) for long-term disposal. The injection well disposes of brine in a narrow target zone over the lowest 1,700 ft (500 m) of the borehole. Mississippian-age limestone takes the majority of injected brine. The in-situ formation water is brine and is therefore not considered a source of potable water. Details on the PVU project background, purpose, and benefits appear in Reclamation's environmental assessment (Bureau of Reclamation, 1997) as well as the Environmental Protection Agency (EPA) injection well permit fact sheet (Environmental Protection Agency, 1997). Figure 3 shows a schematic of the well, including the injection intervals.

PVU has injected brine more or less continuously since 1996, using between one and three constant-rate pumps. In recent years, the wellhead pressure obtained in response to the applied flows has increased. The trend of injection pressures from 2009 to 2012 suggested that the maximum allowable surface injection pressure (MASIP) could be reached within a few years. The MASIP, specified in PVU's operating permit from EPA, was designed to prevent injected brine from breaching a confining layer of salt that lies above the injection target zone and thus prevent contamination of shallow, potentially potable groundwater. In response to a local magnitude (M_L) 4.4 induced earthquake, the flow rate was reduced in early 2013, and maximum injection pressures subsequently decreased. Pressures are expected to gradually increase, even at the reduced flow rate, and may eventually reach the current MASIP. If this occurs, the volume of brine injected annually would need to be further reduced, decreasing the efficiency of operations and making PVU less economically viable.

As a long-term solution, Reclamation is currently evaluating other salinity control alternatives, such as a new injection well or evaporation ponds. While these projects may allow the PVU to continue to operate in the long-term, the design and implementation of a salinity control alternative requires considerable time. Therefore, in the interim, a short-term solution may become necessary. This report summarizes background information relevant to any consideration of whether an increase in the MASIP could be a viable short-term solution to the increasing injection pressures in PVU Injection Well #1. Information presented in this report includes PVU injection history, local geology, geophysical well logging data from the PVU injection well, a

review of the analyses used to design the current MASIP, and a discussion of the possible effects of an increased MASIP on future induced seismicity.

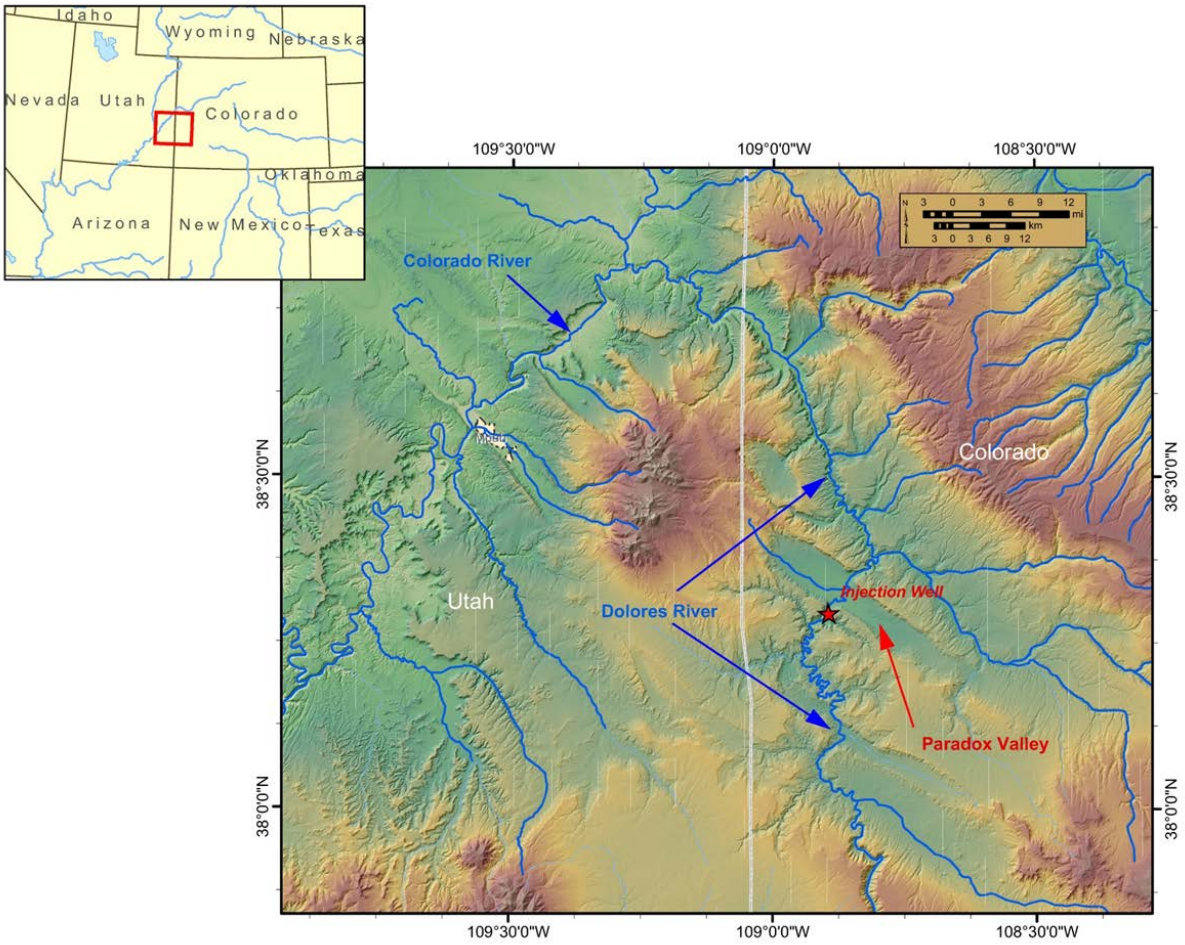

Figure 1 - Location of the deep injection well at Reclamation's Paradox Valley Unit in western Colorado.

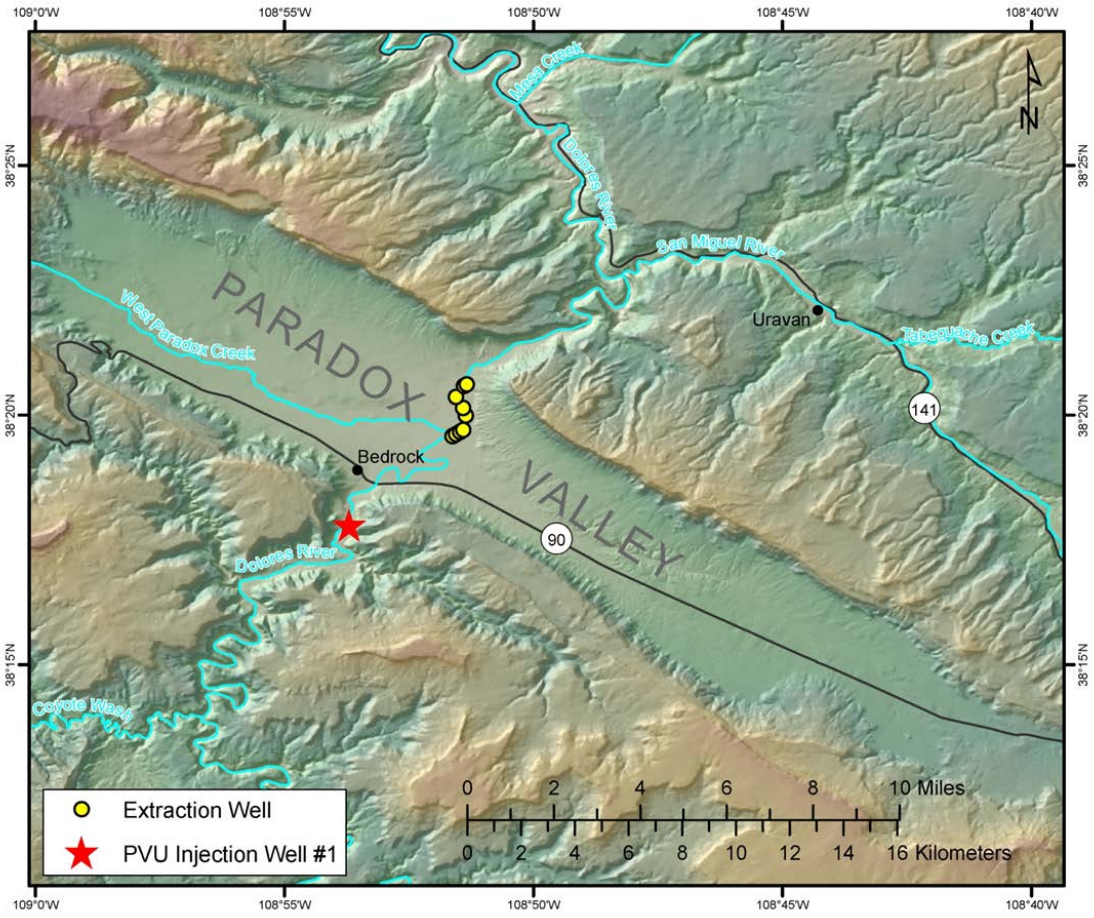

Figure 2 - Location of the Paradox Valley Unit brine extraction wells and PVU Injection Well #1.

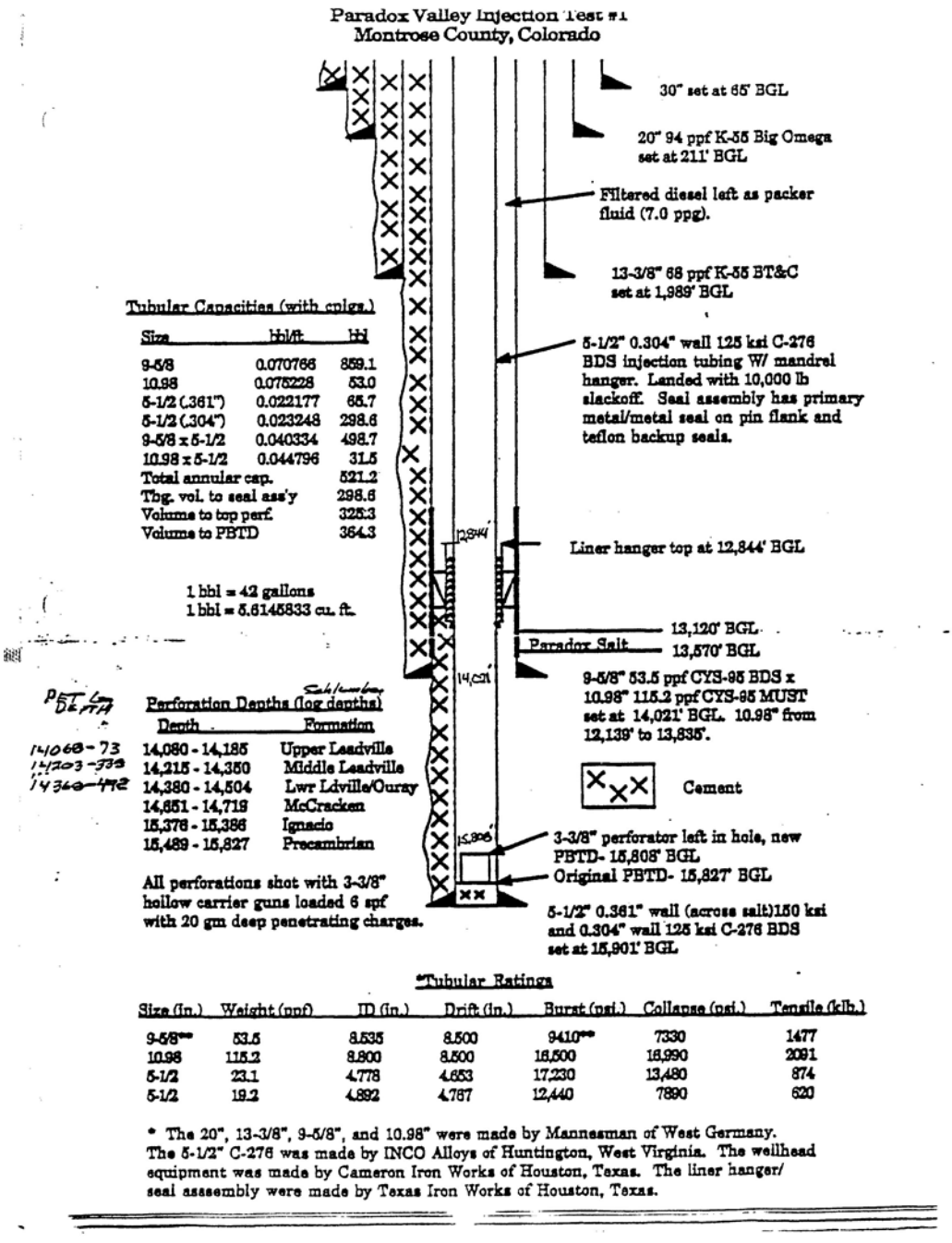

Figure 3 - Schematic diagram of Paradox Valley Injection Test Well No. 1.

2 Project Background

2.1 PVU Injection History

Reclamation began long-term (near-continuous) injection at PVU in 1996, following a series of injection tests conducted between 1991 and 1995. The operational parameters for long-term injection have been changed four times, either in response to large magnitude earthquakes, or in an effort to improve injection economics. These injection phases are briefly summarized below. More detailed descriptions of the injection history are available in other Reclamation reports (Block et al., 2015a; King and Block, 2015). Plots of the daily average injection flow rate, surface injection pressure, and downhole pressure (at a depth of 14,100 ft (4.3 km)) throughout the history of PVU injection operations are shown in Figure 4.

2.1.1 Phase I (July 22, 1996 - July 25, 1999)

During the initial phase of long-term injection, PVU injected at a nominal flow rate of 345 gpm (~1306 l/min), at about 4,950 psi (~34.1 MPa) average surface pressure. To maintain this flow rate, PVU used three constant-rate pumps, each operating at 115 gpm. When the surface pressure approached the MASIP of 5000 psi, PVU shut down one or two injection pumps, thus reducing the injection rate and allowing the injection pressure to drop. These shutdowns occurred frequently and lasted for minutes, hours, or days. The shutdowns resulted in an overall average injection rate for phase I of ~300 gpm (1136 l/min). The injectate during phase I was 70% Paradox Valley Brine (PVB) and 30% fresh water.

2.1.2 Phase II (July 26, 1999 - June 22, 2000)

Following M_L 3.6 and M_L 3.5 induced earthquakes in June and July, 1999, PVU altered injection to include a 20-day shutdown (i.e., a “shut-in”) every six months. The injection pressure and flow rate were the same as during phase I.

2.1.3 Phase III (June 23, 2000 - January 6, 2002)

Immediately following a local magnitude (M_L) 4.3 earthquake on May 27, 2000, PVU shut down injection operations for 28 days. On June 23, 2000, PVU resumed injection with two pumps rather than three. This change decreased the injection flow rate by 33% compared to earlier phases, to 230 gpm (~871 l/min). Accounting for the two 20-day shut-ins per year, the average injection flow rate was approximately 205 gpm (776 l/min), a decrease of about 32% compared to phase I. The 70:30 ratio of brine to fresh water and the biannual 20-day shutdowns were maintained.

2.1.4 Phase IV (January 7, 2002 – January 24, 2013)

In 2001, Reclamation re-evaluated whether dilution of PVB with fresh water prior to injection was still necessary. After this review, Reclamation decided to begin injecting 100% PVB to increase the amount of salt disposed of with the reduced injection rate initialized in Phase III. Injection of 100% PVB began on January 7, 2002 and has been maintained since. The same reduced injection rate as in phase III (230 gpm) and biannual 20-day shutdowns were maintained.

In 2004 the MASIP was raised to 5350 psi. The MASIP was raised to ensure the economic operation of the well. No new data were acquired in order to raise the MASIP, but instead the previous limit of 5000 psi was reevaluated and considered to be well below the previously calculated injection pressure required to breach the confining salt layer (6106 psi). These calculations are documented in section 3.

2.1.5 Phase V (April 17, 2013 – Present)

Following a M_L 4.4 induced earthquake on January 24, 2013 (Block et al., 2014), Reclamation halted injection and reevaluated the seismic hazard associated with PVU operations. Analyses of the seismic and injection data indicated that the potential for inducing large felt events might be reduced by decreasing the long-term average injection pressures (Block and Wood, 2009; Wood et al., 2015). Pressure-flow modeling indicated that reducing the flow rate would reduce wellhead pressures, and forward modeling was used to determine an appropriate flow rate (Wood et al., 2015). In addition, the pressure-flow modeling indicated that changing the injection well shut-in schedule to have shorter, more frequent shut-ins would result in a lower average wellhead pressure, compared to the biannual 20-day shut-ins previously used. Injection was resumed on April 17th, 2013. The nominal flow rate was reduced to 200 gpm with weekly 18-hour shut-ins. The average flow rate during Phase V has been 178 gpm.

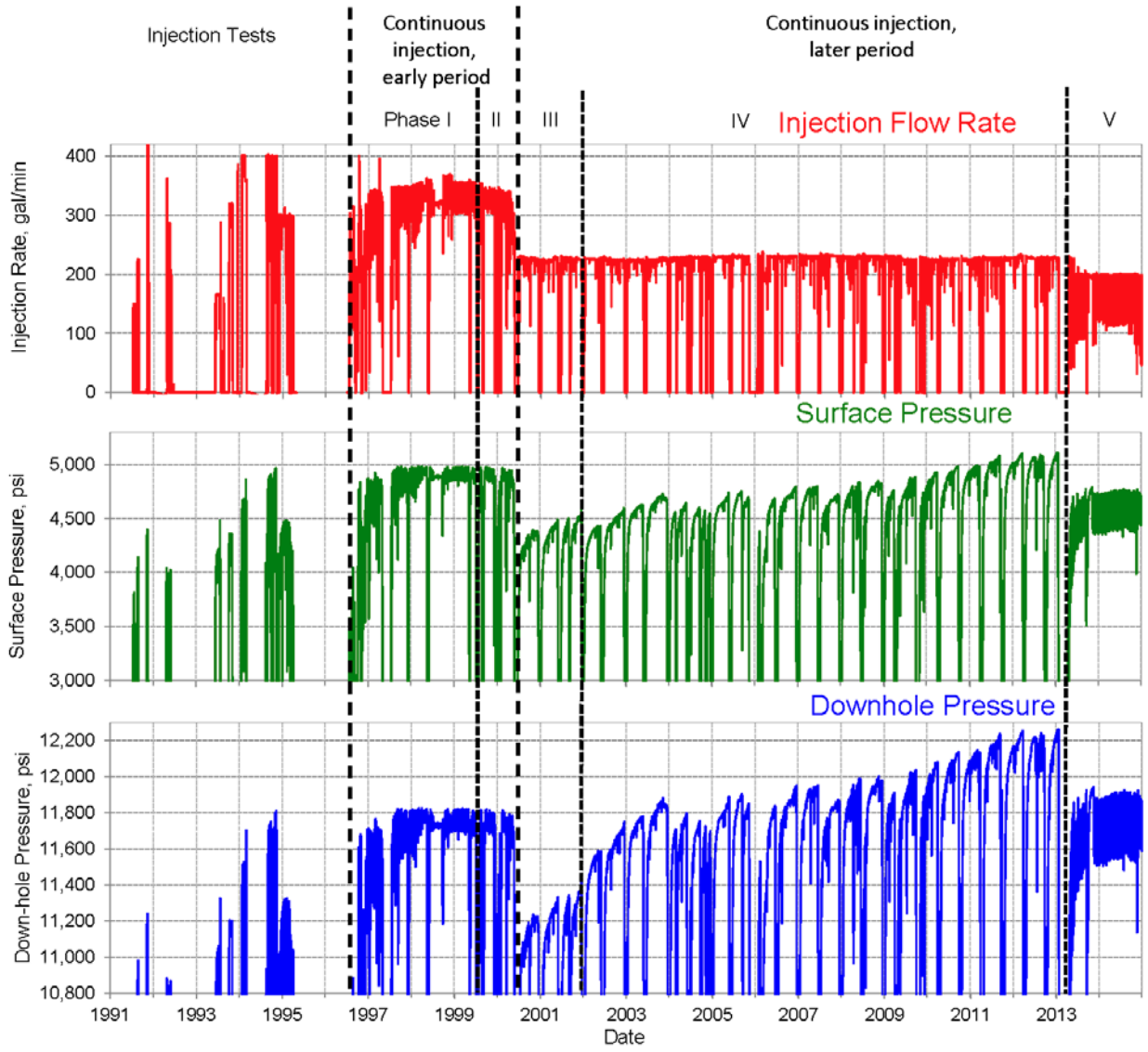

Figure 4 – From Block et al. (2015a). Daily average injection flow rate (top), daily average surface injection pressure (middle), and daily average downhole pressure at 14,100 ft (4.3 km) depth (bottom) during PVU injection operations.

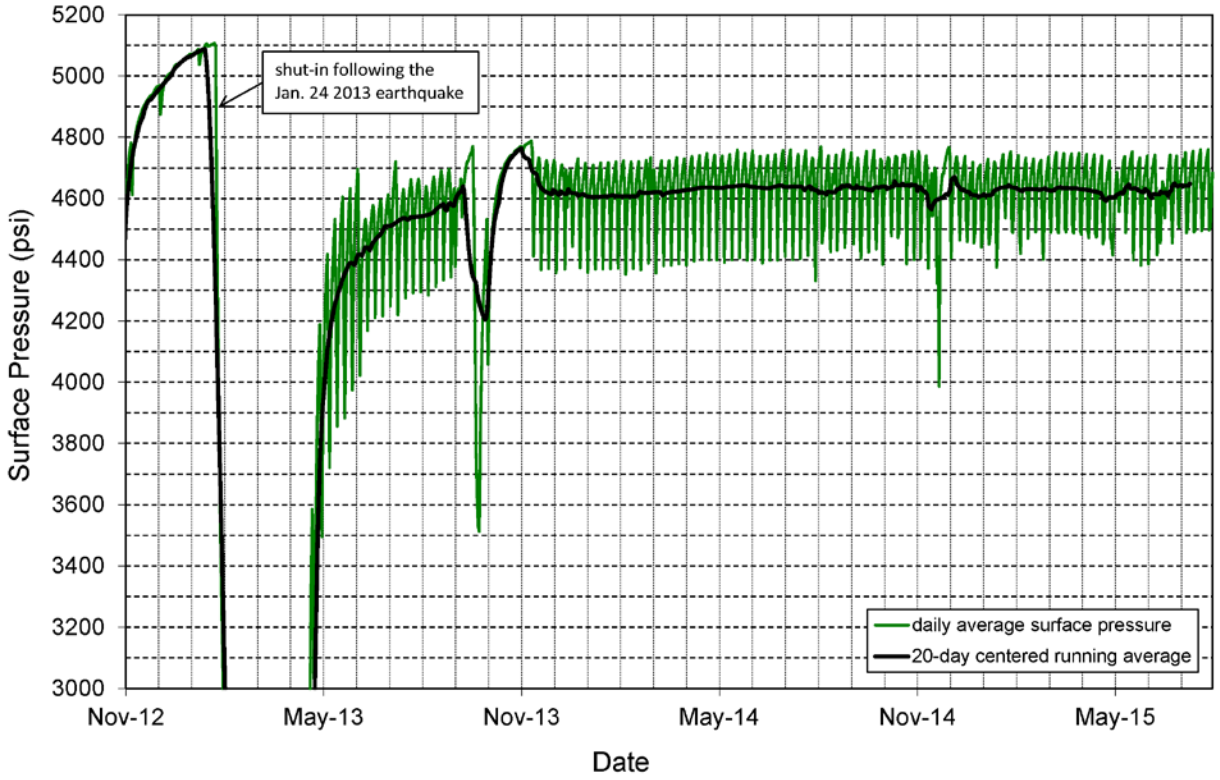

Figure 5 - Daily average wellhead pressures (green) and 20-day centered moving average (black) for end of phase IV and beginning of phase V (November, 2012 – July, 2015). The injection well was shut in for nearly 3 months following a M_L 4.4 induced earthquake on Jan. 24, 2013. Injection resumed on April 17, 2013, with a reduced flow rate and shorter, more frequent shut-ins.

2.2 Injection Pressures

The surface and downhole injection pressures at PVU Injection Well #1 vary considerably over time (Figure 4). After the injection flow rate was decreased by one-third in mid-2000, both the surface and downhole injection pressures dropped by approximately 800 psi and then began to slowly recover. When the injectate was subsequently changed from a 70% brine-30% fresh water mix to 100% brine (January 2002), the increased density of the 100% brine injectate resulted in an immediate increase in the downhole pressure of about 300 psi (Figure 4). By mid-2003, the downhole pressure had reached the same value as prior to the mid-2000 decrease in injection flow rate. The surface injection pressure, in contrast, did not reach the pre-2000 value (just under 5000 psi) until mid-2010 (Figure 4). This distinction between the slow increase in surface injection pressure and rapid increase in downhole pressure is important when considering that the MASIP is designed to prevent the breach of confining layers and therefore it is the downhole pressure, not the injection pressure, which is most relevant.

During injection phase IV (2002-2013), the maximum surface and downhole pressures gradually increased, while the daily average injection flow rate and composition of the injectate remained nearly constant. Short-term fluctuations in injection pressure (for example, in 2004 and late

2005-early 2006) appear to be the result of variation in the frequency and length of shut-ins, both scheduled and unscheduled.

Due to the long shut-in and reduced flow rate following the January 2013 M_L 4.4 event, the surface injection pressure dropped significantly. Since injection operations resumed in April 2013, surface injection pressure has been slowly increasing, with the rate of increase declining over time (Figure 5). The maximum daily average surface injection pressure reached in phase V to date (2013-July 2015) was ~ 4788 psi, reached in November 2013, after an unusually long injection cycle. Although the injection pressures are expected to continue to gradually increase, the rate of increase should further diminish over time (King and Block, 2015).

2.3 Geology

Paradox Valley is located in the northeastern part of Paradox Basin. Rapid subsidence of Paradox Basin during the Mississippian, Pennsylvanian, and Permian Periods (~350 - 250 Ma) accommodated marine intrusion and resulted in the inter-fingering of marine deposits, including evaporates, and terrestrial material shed from the nearby (Uncompahgre) uplifted areas to the northeast (McClure, 2003). The Paradox fold and fault belt, situated in the northern portion of the Paradox Basin, contains several northwest-striking diapiric salt-cored anticlines. These salt-cored anticlines developed as a result of plastic flow of the Pennsylvanian-age Paradox stratigraphic unit. The Paradox unit consists of as much as 85% halite and, according to Huntoon (1988), its deformation is “best imagined as a viscous liquid that can flow in response to imposed stresses”. Subsequent dissolution of salt beneath the crests of some of the anticlines resulted in down-faulting and the development of grabens, or salt valleys (Gutiérrez, 2004, Nuccio and Condon, 1996). Paradox Valley developed as a result of structural collapse along the crest of one of these salt-cored anticlines and is bounded by nearly vertical normal faults.

Paradox Valley and the surrounding mesas contain rocks spanning Precambrian to mid-Cretaceous time (>570 to approximately 90 Ma) (Block et al., 2012). The Precambrian basement rock consists of granite, schist, gneiss, and pegmatite. Overlying the Precambrian rock is a series of sedimentary units deposited primarily in marine or near shore environments. These layers include sandstones, siltstones, shales, conglomerates, limestones, dolomites, and evaporates (Block et al., 2012). A geologic cross section from King et al. (2014), through the injection well and approximately perpendicular to Paradox Valley, is presented in Figure 6. PVU Injection Well #1 is sited on the Triassic-age Chinle Formation. The stratigraphy of the underlying formations is described in Table 1. Depths of geologic units encountered in this well are included in the table and are relative to the local ground surface elevation of 4996 ft (1523 m). Descriptions of the rock units are taken from several sources (see footnote no. 2 in the table). Further details of the local geology can be found in Block et al. (2012) and King et al. (2014).

The Mississippian Leadville formation is the primary target reservoir for PVU brine injection (Bremkamp and Harr, 1988). The Leadville formation was selected due to its relatively high permeability, largely the result of an extensive system of fractures in the rock. The upper Precambrian was originally considered a secondary injection target, and some of the Cambrian and Devonian units were also considered to have some injection potential (Bremkamp and Harr, 1988). PVU Injection Well #1 contains several perforated zones spanning the interval from the

Leadville formation to the Precambrian (Figure 3). However, early flow profiles indicate that the Leadville formation accepts the majority of fluid (Envirocorp, 1995), and over time the deeper perforations have been covered with fill from precipitation of sulfur in the wellbore (Subsurface Technology, 2001). The overlying Paradox salt formation is the primary confining layer.

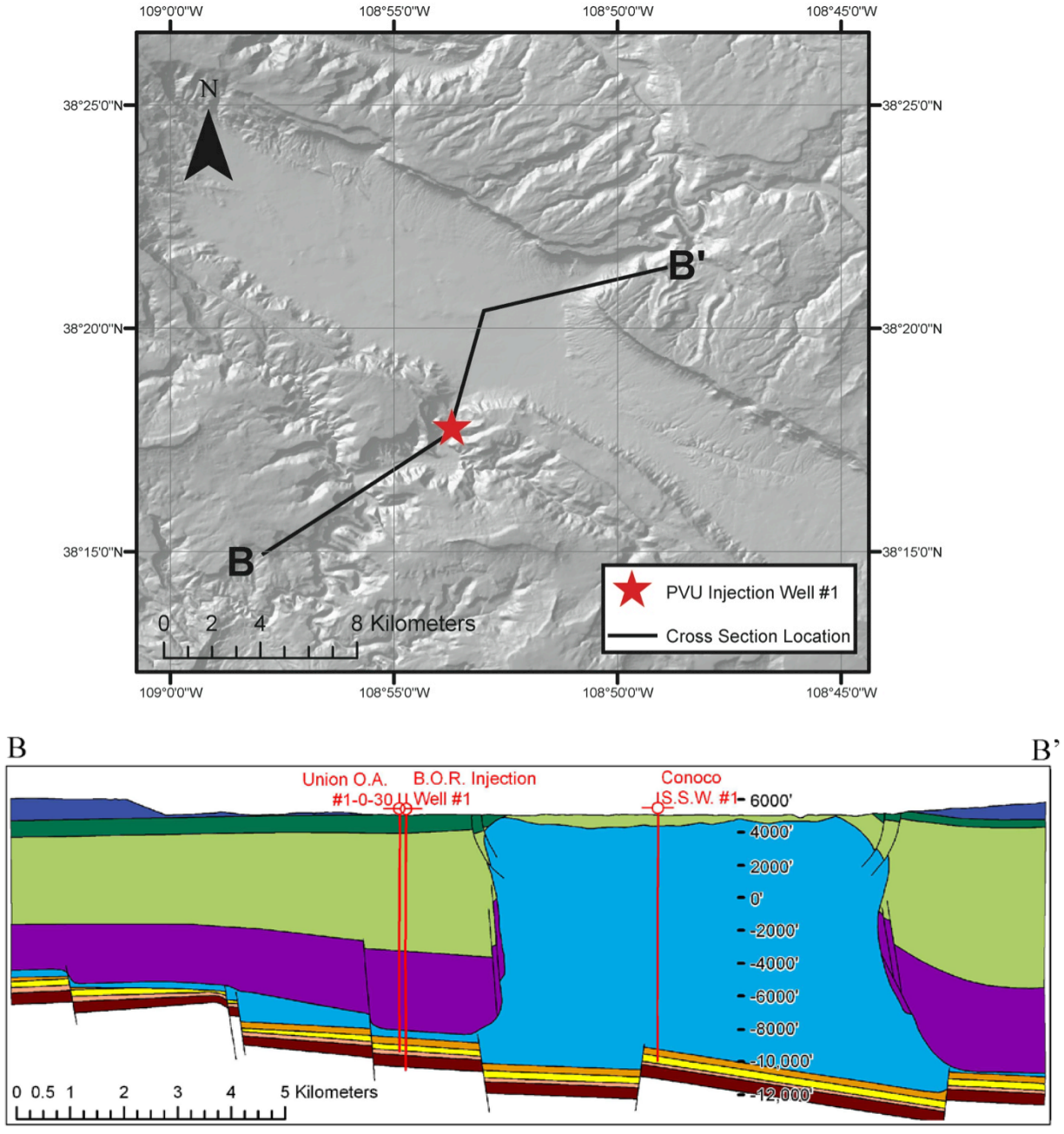

Figure 6 – (Top) Location of geologic cross section B-B'. (Bottom) Cross Section B-B' digitized and modified from Bremkamp and Harr (1988) and taken from King et al. (2014). There is no vertical exaggeration.

Table 1 - From King et al. (2014). Stratigraphy at the PVU well.

Stratigraphic Unit	Depth[1]	Description[2]
CRETACEOUS[3] (145-65 Ma)		
Mancos Shale	Above elevation of wellhead	Dark gray to black, soft, fissile marine shale with thin sandstone beds at various horizons.
Dakota Sandstone		Friable to quartzitic fluvial sandstone and conglomeratic sandstone with interbedded carbonaceous nonmarine shale.
Burro Canyon Fm.		Fluvial sandstone and conglomerate interbedded with lacustrine siltstone, shale, and mudstone, and thin beds of impure limestone.
JURASSIC (205-145 Ma)		
Morrison Fm.	Above elevation of wellhead	Fluvial and lacustrine shale, mudstone, and sandstone; local thin limestone beds.
Summerville Fm.		Sandy shale and mudstone of terrestrial origin.
Entrada Sandstone		Fine- to medium-grained, massive, and cross-bedded eolian sandstone; basal few feet may consist of red siltstone and fine-grained sandstone and is sometimes referred to as the Carmel Formation.
Navajo Sandstone		Fine-grained, cross-bedded eolian sandstone.
TRIASSIC (255-205 Ma)		
Kayenta Fm.	Above elevation of wellhead	Irregularly interbedded fluvial shale, siltstone, and fine to coarse-grained sandstone.
Wingate Sandstone		Fine-grained, massive, thick-bedded and prominently cross-bedded eolian sandstone.
Chinle Fm.	0 (at surface)	Siltstone interbedded with lenses of sandstone and shale, limestone-pebble and shale-pellet conglomerate, with lenses of grit and quartz-pebble conglomerate near base. Terrestrial depositional environment.
Moenkopi Fm.	390	Sandy shale/silty sandstone with some conglomerate present. Marine and terrestrial depositional environment.
PERMIAN (298-255 Ma)		
Cutler Fm.	1,140	Fluvial arkose and arkosic conglomerate, with some sandy shales; deposited in alluvial fans.
PENNSYLVANIAN (322-298 Ma)		
Hermosa Group – Honaker Trail Fm.: Upper Honaker Trail	8,313	Limestone/sandstone/siltstone; deposited in marine conditions.
La Sal	12,006	Limestone/dolomite; some silty limestone, oolitic limestone, and algal limestone present.

Lower Honaker Trail	12,082	Limestone/sandstone/siltstone; deposited in marine conditions.
Hermosa Group – Paradox Fm.: Ismay 1st Main Salt 2nd Main Salt Base Salt – Lower Paradox	 12,350 12,839 13,104 13,497 13,566	 Resulted from intermittently closed marine environment. Limestone, stacked algal carbonate mounds and other shallow-water carbonates and dolomites. Dolomite/salt; intermittently closed marine environment. Salt/anhydrite/shale; intermittently closed marine environment. Shale/anhydrite/(minor) limestone; intermittently closed marine depositional environment.
Hermosa Group – Pinkerton Trail Fm.	13,693	Shales/anhydrites/siltstone/(minor) limestones; dark colored shales, limestone formed by marine invasion.
Molas Fm.	13,944	Shale/siltstone/claystone; regolith/soil (*terra rosa*) de-veloped on the karst surface of the Leadville formation after a period of extensive weathering and erosion.
MISSISSIPPIAN (355-322 Ma)		
Leadville Fm.	13,984	Limestone/dolomite. Lower unit (Kinderhookian-age) stromatolitic dolomite, lime mudstones, pelletal lime mudstones; deposited in intertidal to subtidal environments. Upper unit (Osagean-age) fossiliferous pelletal and oolitic limestone, and lime and dolomitic mudstone.
DEVONIAN (416-355 Ma)		
Ouray Fm.	14,400	Limestone—lime mudstone, pelletal lime mudstone and skeletal limestone that is locally dolomitized; formed in quiet-water marine environment.
Elbert Fm.	14,440	Sandstone/shales/shaly dolomites.
McCracken Fm.	14,607	Sandstone with occasional interbeds of sandy dolomite; transgressive depositional environment.
Aneth Fm.	14,681	Dolomite/shale; dense, argillaceous sequence.
CAMBRIAN (540-488 Ma)		
Lynch Fm.: Upper Lynch Shale Lynch Limestone Lower Lynch	 14,763 14,835 14,928	 Sandstone/interbedded shale, dolomite, limestone. Limestone. Shale.

Shale		
Muav Fm.	14,988	Limestone.
Bright Angel Fm.	15,103	Shale.
Ignacio Fm.	15,246	Sandstone, sometimes referred to as quartzite; transgressive depositional environment.
PRECAMBRIAN (>540 Ma)		
Precambrian	15,446	Described regionally as granitic rock with well-developed northwest and northeast orthogonal fracture systems; identified in PVU Injection Well #1 as moderately metamorphosed diorite-gabbro schist.

[1]Depths are taken from the geologic drill log of PVU Injection Well #1 (Harr, 1988). Depths are relative to the ground surface elevation (4996 ft) and have been corrected for borehole deviation.
[2]Descriptions are taken from: Bremkamp and Harr (1988), Campbell (1981), Doelling (1988), Williams (1964), and Nuccio and Condon (1996).
[3]Ages from Walker and Geissman (2009).

3 MASIP Calculations

In this section, we summarize information from several early PVU reports relevant to the MASIP calculations for PVU Injection Well #1. Calculations documented in the existing reports rely heavily on interpretations of geophysical well logs from the injection well. A brief summary of the geophysical well logs from the injection well, with emphasis on those logs that provide data directly relevant to the MASIP calculations, is provided in section 3.1. In section 3.2, we summarize calculations that were performed prior to completion of the PVU well and injection testing to assess the confining ability of the Paradox formation. We also examine the dependence of that analysis on the plasticity of the Paradox salt. Next, we review the MASIP calculations documented in the injection permit from EPA (section 3.3). Lastly, we review the criteria that must be met if Reclamation were to seek approval for an increase in the current MASIP for the PVU injection well (section 3.4).

3.1 Relevant PVU Well Logging

Open-hole logging was performed in the injection well in three stages as the borehole was drilled: (1) after drilling the shallow hole (90 ft – 2012 ft) (Dewan, 1987a), (2) after drilling the intermediate hole (2020 ft – 14050 ft) (Dewan, 1987b), and (3) after drilling the deepest portion of the well, referred to as the liner hole (14050 ft - 15950 ft) (Dewan, 1987c; Dewan, 1988a). These stages correspond to progressively decreasing borehole diameter (Figure 7). Final well logs, composed of a composite of these individual runs, were constructed after all open-hole logging was completed (Dewan, 1988b).

Logging from the intermediate and liner holes provides data for the MASIP calculations. These two stages span most of the borehole, including the Paradox Salt, considered the major confining layer, and the Leadville formation, the primary injection target reservoir. Descriptions of the acquisition and processing of the geophysical logging data from these two sections of the borehole are presented below. These descriptions, including the qualitative evaluations of the data quality and the results derived from the data processing, are taken from the relevant original well log reports. We did not re-evaluate the geophysical well logging data or perform additional analyses of the data when writing this report.

3.1.1 Intermediate Hole Logging (14,050-2,020 ft; upper Leadville - Cutler):

Open-hole logging of the intermediate hole (14,050 – 2020 ft depth) was performed by Schlumberger and documented by Dewan (1987b). All descriptions of the field-recorded and computed well logs presented in this section are summarized from Dewan (1987b).

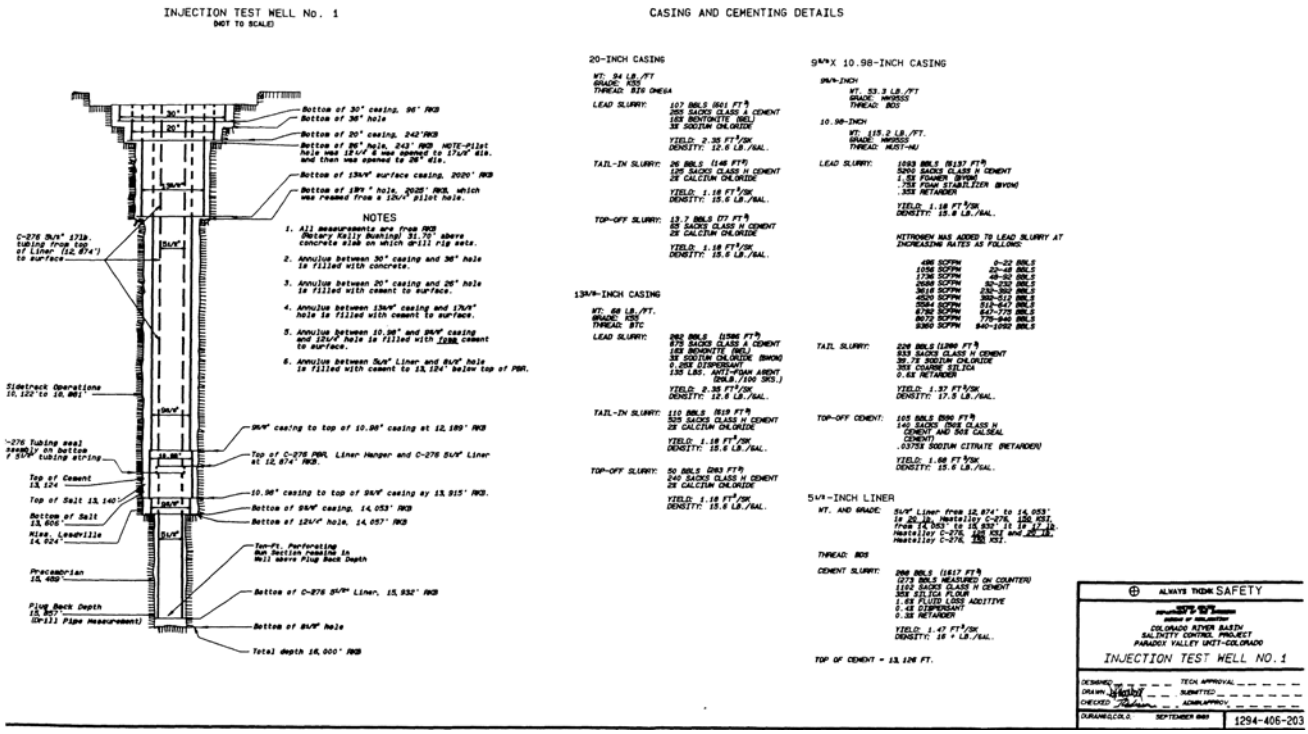

Figure 7 – Casing and cementing details of PVU Injection Well #1.

Field Recorded Logs:

Schlumberger performed four successful well log runs in the intermediate portion of the well:

Run 1: Dual Laterlog (DLL), Microspherically Focused (MSFL), Dual Caliper, Gamma Ray (GR)

Resistance of the tool to being pulled up the well, as evidenced by multiple periods of increased tension on the wireline, were experienced between 12,470 ft and 11,527 ft during this run. The arms of the caliper logging tool were closed between ~11,527 ft and ~10,000 ft because of the difficulty with getting the tool through this section of the hole. These problems occurred above the major salt layer and therefore did not affect data in the region of greatest interest. Dewan (1987b) found the borehole to be significantly out-of-round, typically 12 ½" in one direction and 14"-16" in the other. The deep laterolog resistivity curve (LLD) indicated highly resistive salt beds; the shallow curve (LLS) was not useful because of the effects of large borehole diameter and salt-saturated drilling mud. Dewan (1987b) considered the gamma ray curve to be good for correlation and indicative of some zones rich in potassium minerals. The MSFL was only recorded across the lowest 500 ft of the intermediate hole (~13,550 – 14,050 ft depth) because of tool damage.

Run 2: Borehole Compensated Sonic (BHC), GR

Dewan (1987b) reported the quality of the sonic log from this run to be excellent, excluding short sections at 13,455 ft and 8,610 ft where abnormally large borehole washouts caused cycle skipping. A sonic-derived porosity, ϕ, was calculated using the following equation:

$$\phi = 0.625\left(1 - t_{ma} / t\right) \qquad (1)$$

where t is the sonic slowness (μsec/ft) and t_{ma} is the matrix slowness, set to 49 μsec/ft, considered appropriate for limestone. Since the actual lithologies are variable, the sonic porosity log is only approximate and is most accurate for the limestone sections. This relation does not hold for salt formations, in which a salt porosity of zero was assumed (Dewan, 1987b).

Run 3: Digital Sonic, GR

This run recorded complete sonic waveforms from 12,986 to 14,050 ft. The sonic logger consisted of 10 receivers spaced at 6" intervals. The quality of the sonic log was considered excellent. Compressive and shear velocities were calculated from this record.

Run 4: Stratigraphic High-Resolution Dipmeter (SHDT), GR

This run had many mechanical issues, including the logging tool sticking in the hole and the winch breaking. The quality of the run was therefore poor, but still good enough to extract structural dip at depths below 10,500 ft.

Computed Logs:

The digital sonic data from run #3 was processed using a slowness-time-coherence (STC) algorithm. Computed compressive and shear slownesses were used to calculate Poisson's ratio using the following relation:

$$\mu = 0.5\frac{\left(\left(\frac{t_s}{t_p}\right)^2 - 2\right)}{\left(\left(\frac{t_s}{t_p}\right)^2 - 1\right)} \qquad (2)$$

where μ is Poisson's ratio (dimensionless), t_p is the compressional-wave slowness (μs/ft), and t_s is the shear-wave slowness (μs/ft) (Dewan, 1987b).

A sonic-derived density was calculated from the BHC sonic log using the equation

$$\rho = 1.63 + {}^{52.8}\!/_{t} \quad (3)$$

below 9,300 ft and the equation

$$\rho = 1.61 + {}^{57.2}\!/_{t} \quad (4)$$

above 9,300 ft, where ρ is the density (g/cm^3) and t is the compressional-wave slowness (μs/ft). The density calculations were considered appropriate for carbonates below 9,300 ft and appropriate for sandstones above 9,300 ft (Dewan, 1987b). Areas with a resistivity greater than 20,000 ohm-m and slowness greater than 54 μs/ft were considered salt, and the density for these areas was set to 2.16 g/cm^3. Densities were also calculated from a BHC sonic log acquired in the surface hole below 240 ft depth and merged with the results from the intermediate hole. To extrapolate the density log to the ground surface, a density of 2.4 g/cm^3 was assumed above 240 ft.

The calculated densities were used to compute the overburden pressure P_0 as a function of depth. An extra 1,000 ft of overburden was added to the pressure calculations due to the fact that the well bottom is 1,200 ft laterally offset from the wellhead location, below a large mesa. The extra overburden was assumed to have a density of 2.4 g/cm^3. The intermediate hole bottom (14,050 ft depth) overburden pressure was calculated to be 16,400 psi, which corresponds to an overburden pressure gradient of 1.167 psi/ft. Pore pressure P_P was also calculated assuming the water column extended 1,000 ft above the ground surface at the wellhead using a pore-pressure gradient of 0.442 psi/ft (Dewan, 1987b).

These results, combined with the calculated Poisson's ratio, were used to calculate the fracture closure pressure (FP_{CL}) as a function of depth:

$$FP_{CL} = mP_o + P_p(1-m) \quad (5)$$

where $m = \mu/(1-\mu)$. The fracture closure pressure is the fluid pressure required to open a preexisting fracture in the rock. Horizontal stress was assumed isotropic. The fracture initiation pressure (FP_{IN}), the pressure required to initiate fracture of intact rock, was then computed as a function of depth following:

$$FP_{IN} = 2FP_{CL} - P_p \quad (6)$$

These calculations assumed no tensile strength in the rock and no incremental invasion of fluid during fracturing and were therefore considered conservative (Dewan, 1987b). Calculations accounting for tensile strength were also computed, but Dewan (1987b) considered the results from those calculations to be less reliable than the results presented here. Fracture closure and initiation pressure gradients were computed by dividing FP_{CL} and FP_{IN} by the depth. The results

indicated FP_{IN} gradients ranging from 0.8-1.2 psi/ft through most of the depth interval from 14,050 to 13,000 ft. FP_{CL} gradients were 0.6-0.8 psi/ft in the same interval. The salt fracture closure and initiation pressure gradients were calculated to be 0.72 psi/ft and 0.97 psi/ft, respectively. The computed fracture closure and initiation pressure curves are included on the mechanical properties log (Dewan, 1988b).

3.1.2 Liner Hole Logging (15,950-14,050 ft) (Precambrian – upper Leadville):

The liner hole section spans the upper Leadville formation through the Precambrian basement (15,950 to 14,050 ft depth). The well logging performed in the liner hole was more extensive than that performed in the intermediate hole. In addition to the same types of logs as acquired in the intermediate hole, the following additional logs were acquired in the liner hole: litho-density, compensated neutron, spectral gamma ray, borehole televiewer, and a suite of geochemical logs (Dewan, 1987c). According to Dewan (1987c), the quality of the logs in this portion of the borehole was sub-par as a result of borehole washouts. Tool malfunctions and the need to ream or clean out the borehole several times because of ledges encountered in the hole also caused difficulties and resulted in some logs being acquired with multiple runs to cover the entire depth range desired. In all, 13 well logging runs were completed by Schlumberger. These individual runs are documented in Dewan (1987c).

The analyses performed on the well logs from the liner hole largely focused on identifying high porosity injection intervals (Dewan, 1988a). As for the intermediate borehole, fracture initiation and closure pressure gradients were also computed, and these data partially form the basis of the MASIP calculations. Below we summarize information presented in the original well logging interpretation report for the liner hole (Dewan, 1988a). We have not performed any additional review or analyses of the well logging data or results.

Field Recorded Logs:

Dual caliper logs, run above a depth of 15,320 ft, indicated that the borehole was oblong. The minimum borehole diameter was generally close to the 8.5" bit size, while the maximum well diameter ranged from 10" to over 20". This suggested to Dewan (1988a) that substantial tectonic stresses were present at these depths.

A combined dual laterolog – micro-spherically focused well log was run to obtain information on formation porosities. The laterolog deep resistivity curve (LLD) was the only reliable curve obtained and was used to calculate formation porosities. The shallow laterolog and MSFL curves were unreliable due to borehole washouts and pad standoff. The LLD curve was considered a good indicator of porosity given the absence of shale and hydrocarbons (Dewan, 1988a). Porosity (ϕ) was estimated using the resistivity measured from the LLD, $Rlld$, using the equation:

$$\phi = \frac{0.15}{\sqrt{Rlld}} \qquad (7)$$

The results indicated porosities of 1% to 5% (with average values of 2% and 3%) in two intervals in the upper and middle Leadville formation. A few zones with comparable porosity were found below the Leadville, but according to Dewan (1988a) the presence of shale may have biased the results.

A litho-density- (LDT) – compensated-neutron (CNL) - GR log also experienced problems as a result of borehole washouts and borehole eccentricity. As a result, Dewan (1988a) considered the data unreliable over about one-third of the depth range logged. In the reliable sections, the density and neutron logs indicated porosities of 0% to 6% (with averages of 4% and 5%) in the same two upper-mid Leadville intervals identified from the LLD log. Areas of comparable porosity in deeper formations identified from these logs corresponded less closely to those observed in the LLD log; however, both sets of logs indicated intervals in the upper Precambrian with porosities of about 2% to 5%.

An 8-receiver digital sonic log was also acquired and used to derive porosity. In general, Dewan (1988a) considered the P- and S-wave slowness measurements to be good, with the exception of a few washed out intervals. Porosity (ϕ) was calculated using the relation:

$$\phi = \left(t - t_{ma}\right) / \left(t_f - t_{ma}\right) \qquad (8)$$

where t is the recorded P-wave slowness (μs/ft), t_{ma} is the slowness of the matrix, assumed to be 47.6 μs/ft in limestone, and t_f is the fluid slowness, assumed to be 190 μs/ft. Calculated porosities agreed broadly with those derived from the LLD and LDT-CNL logs, suggesting porosities of ~2% in the upper-mid Leadville and ~3% in some upper Precambrian intervals. Fractured areas were suggested based on a decrease in shear-wave amplitudes. Generally these intervals were small (< 20 ft), and their validity was questionable (Dewan, 1988a).

A borehole televiewer log was run, but the images contained high-amplitude signals as a result of the ellipticity of the well. Interpretations from formation microscanner, stratigraphic dipmeter, and geochemical logs were either used as quality control or as input to the computed logs.

Computed Logs:

Because of the roughness of the borehole, the structural dip data showed a lot of scatter in both magnitude and direction. However, Dewan (1988a) considered the structural dip to be well resolved from 14,740 to 15,230 ft depth. Combining this information with the dip log from the intermediate borehole, Dewan (1988a) concluded that the structural dip is largely constant in the bottom 2500 ft of the well, with formations dipping about 5° to the northeast.

A fracture identification log (FIL) was also computed from the dipmeter data. The FIL log indicates three fractured zones, two in the upper-mid Leadville and one in the upper Precambrian. These intervals correspond to depths identified as having a few percent porosity by the laterolog deep resistivity, density, neutron, and sonic logs. The fractured zones within the Leadville appear to coincide with the presence of dolomite (Dewan, 1988a).

The 8-receiver digital sonic log was processed using an STC algorithm. Despite the poor borehole conditions, Dewan (1988a) considered the P- and S-wave velocities to be reliable over most depths. The V_P/V_S ratios were reported to range from 1.6 to 2.0, with the exception of a few intervals where the computed V_P/V_S was as high as 2.2 (Dewan, 1988a). The anomalously high V_P/V_S values are not confirmed by the truck-processed sonic log and may not be robust.

A mechanical properties log was computed following a similar procedure as for the intermediate hole. A difference in these computations was the use of bulk density computed from the LDT log rather than from the sonic log. At some depths, large borehole washouts biased the LDT log and resulted in an anomalously low computed density value. To compensate for this problem, the density was set to 2.4 g/cm^3 at any depth where the computed density was below that value. Overburden pressure (psi) was then calculated as a function of depth *z* (ft) using the equation:

$$P_o(z) = P_o(14,050) + 0.433 \int_{14,050}^{z} \rho(z)\, dz \qquad (9)$$

where $P_o(14,050)$ is the overburden pressure calculated from the intermediate hole logging at 14,050 ft depth (~16,500 psi), ρ is the bulk density (g/cm^3) from the LDT log in the liner hole, and 0.433 is a factor needed to convert units (Dewan, 1988a). Pore pressure (psi) was calculated as a function of depth *z* (ft) with the equation:

$$P_p(z) = 6{,}160 \text{ psi} + 0.442 \text{ psi/ft} \int_{14,100}^{z} dz \qquad (10)$$

where 6,160 psi is the pore pressure directly measured by a drill stem test at 14,100 ft depth and 0.442 psi/ft is the assumed gradient for the formation water. FP_{IN} and FP_{CL} were calculated as for the intermediate hole (assuming no tensile strength in the rock and no incremental invasion of fluid during fracturing). Above 14,650 ft depth (in the Leadville and underlying Devonian units), computed FP_{IN} gradients were similar to those measured in the intermediate hole, ranging from 0.8 to 1.1 psi/ft. In some sections below 14,650 ft depth containing more siliceous materials, FP_{IN} gradients were as low as 0.5 psi/ft. FP_{CL} gradients were generally ~0.3 psi/ft less than the FP_{IN} gradients. FP_{IN} was recalculated accounting for tensile strength, but Dewan (1988a) considered those calculations to be less reliable than the calculations using zero tensile strength.

3.2 Evaluation of the Confining Layer

Prior to completion of the PVU injection well, the confining ability of the Paradox salt was evaluated to ensure that vertical fractures in the target injection formations would not propagate through the confining layer. According to Dewan (1988c), once the injection zone was broken down, the critical factor that controlled vertical fracture propagation was the difference in closure

pressures between the injection interval and the overlying or underlying formations. In the case of PVU, Dewan (1988c) considered this to be the difference between the closure pressure of the Leadville formation (14,080 – 14,350 ft) and that of the overlying salt section of the Paradox formation (13,140 – 13,600 ft). The closure pressures computed from the geophysical well log data were used as estimates of the minimum horizontal stresses in these formations.

Relying on the computed mechanical properties log, Dewan (1988c) found that the minimum horizontal stresses (FP_{CL}) in the Leadville formation ranged from 9,000 to 11,000 psi (corresponding to gradients of 0.65 – 0.8 psi/ft). The salt was determined to have similar calculated minimum horizontal stresses of 9,000 to 10,000 psi (gradients of 0.7-0.8 psi/ft) on the mechanical properties log. However, Dewan (1988c) stated that due to the ability of the salt to creep, the minimum horizontal stress in the salt is equal to the overburden pressure (i.e., an isotropic stress state in the salt layer equal to the lithostatic stress should be assumed). Dewan (1988c) argued that since the mechanical properties log was computed from measurements recorded at 20 khz, the salt did not have adequate time to creep, which resulted in underestimating the minimum horizontal stress. Instead, Dewan (1988c) suggested the use of the overburden pressure at the depth of the salt, 14,500 psi (computed from geophysical logs in the intermediate hole), as the minimum horizontal stress for the salt. Therefore, according to Dewan (1988c), the minimum difference in the closure pressures between the Leadville and salt formations was 3,500 psi (14,500 psi – 11,000 psi).

Next, Dewan (1988c) computed the effective confining differential (ECD). The ECD takes into account the pressure difference from the hydrostatic head in the two zones. Dewan (1988c) computed the hydrostatic head difference (HHD) between the Leadville and salt to be ~400 psi ($(14,200\text{ ft.} - 13,300\text{ ft.}) \times 0.46\text{ psi/ft}$). Hence, Dewan (1988c) determined the ECD to be $\geq$ 3,900 psi.

In response to concerns about the assumption that the horizontal stress in the salt is equal to the overburden pressure, various experts in the field were consulted (Dewan, 1988d). The consensus was that the assumption of isotropic stress in the salt was correct, and therefore the minimum *ECD* value of 3900 psi was considered valid (Dewan, 1988d).

Dewan (1988d) suggested that the fracture propagation modeling in use at that time (using the *FracHite* computer program by Schlumberger) be performed assuming a range of Poisson ratios in the salt in order to understand the sensitivity of the results on the assumption of isotropic stress. This work does not appear to have been completed. However, it is possible to evaluate the sensitivity of the *ECD* calculation on the assumption of isostatic stress in the salt. Substituting the values used by Dewan (1988c) (overburden pressure in salt = 14,500 psi, depth of salt = 13,300 ft, pore pressure gradient = 0.46 psi/ft) into equation (5), we calculate the fracture closure pressure in the Paradox salt as a function of Poisson's ratio (Figure 8a). Subtracting the largest closure pressure value for the Leadville (11,000 psi) and adding the HHD value given above (400 psi) then provides a minimum estimate of the *ECD* as a function of Poisson's ratio (Figure 8b). The results show that if the Poisson's ratio of the salt is less than ~0.33, the minimum estimate of ECD is less than or equal to zero. This demonstrates that the confining ability of the salt, as evaluated using differences in fracture closure pressures, is highly dependent on the assumption that the state of stress in the salt is isotropic (i.e., Poisson's ratio is close to 0.5).

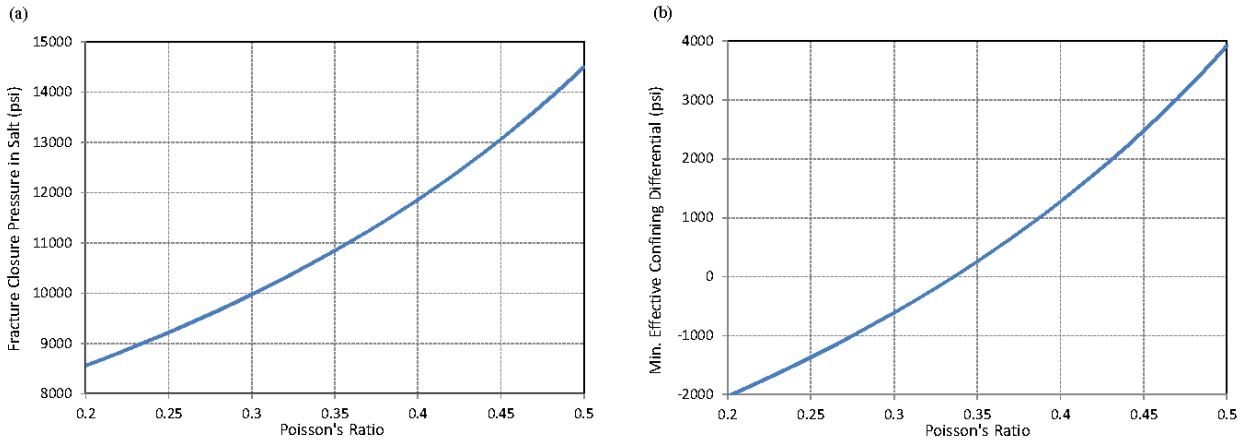

Figure 8 – (a) Fracture closure pressure in Paradox salt and (b) Minimum effective confining differential as a function of Poisson's ratio.

3.3 MASIP Calculations

Prior to determining the appropriate MASIP, the surface injection pressures required to open pre-existing fractures within the Leadville were examined. Due to the fact that the permeability of the Leadville is largely the result of a well-developed fracture system rather than primary porosity (Bremkamp and Harr, 1988), it was deemed advantageous to inject at downhole pressures above the Leadville fracture closure pressure so that preexisting fractures would be opened (Environmental Protection Agency, 1997). EPA calculated the corresponding injection pressure at the ground surface (accounting for friction loss in the well tubing), referred to as the maximum surface injection pressure ($MSIP$), following the equation:

$$MSIP = \left(F_{gradient} - 0.433\ \text{psi/ft} \times SG \right) d + \Delta p_{fric} \qquad (11)$$

where $F_{gradient}$ is the fracture closure pressure gradient in the Leadville formation (0.685 psi/ft), SG is the specific gravity of the brine (1.167), d is the depth to the top perforation (14,080 ft), and Δp_{fric} is the friction loss in the well tubing (psi) from the ground surface to the top perforation (Environmental Protection Agency, 1997). The value 0.433 psi/ft comes from a typical pressure gradient of fresh water.

The *MSIP* was computed using values of Δp_{fric} estimated by Envirocorp, Reclamation, and EPA. EPA estimated a frictional loss of 915 psi, assuming a loss of 65 psi per 1000 ft (Environmental Protection Agency, 1997). Reclamation's estimated frictional loss was nearly an order of magnitude smaller, 135 psi, which was calculated using the equation:

$$\Delta p_{fric} = \frac{SG \times Q^2}{1369.38} \qquad (12)$$

where SG is the specific gravity of the PVU brine (1.167) and Q is the injection flow rate (400 gallons/minute) (Environmental Protection Agency, 1997). Envirocorp calculated a similar frictional loss of 111 psi for a flow rate of 400 gallons/minute following the equation:

$$\Delta p_{fric} = 0.433 \rho_{brine} f \frac{0.03112 L Q^2}{d^5} \qquad (13)$$

where ρ_{brine} is the density of the brine in g/cm^3, L is the tubing length (14,080 ft), Q is the injection flow rate (400 gal/min), d is the inner diameter of the tubing in inches, and f is a dimensionless friction factor given by:

$$\frac{1}{\sqrt{f}} = -2 \log_{10} \left[\frac{\varepsilon}{3.7 d/12} + \frac{2.51}{R\sqrt{f}} \right] \qquad (14)$$

(Envirocorp Services and Technology Inc., 1995; Environmental Protection Agency, 1997). R is the Reynold's number (dimensionless), and ε is the pipe roughness in feet. The resulting *MSIP* values are: 3445 psi (EPA), 2655 psi (Reclamation), and 2644 psi (Envirocorp) (Environmental Protection Agency, 1997).

In an EPA injection permit, a maximum allowable surface injection pressure is established to ensure that injection pressures remain low enough to prevent the propagation of new and existing fractures vertically through the confining layer and into formations that contain underground sources of drinking water. This permitted limit on the surface injection pressure, the MASIP, was calculated for PVU Injection Well #1 considering the estimated fracture initiation pressure gradient for the confining Paradox salt, 0.97 psi/ft (from Dewan 1987b). The 0.97 psi/ft value relied on Poisson's ratios and densities derived from the sonic well log in the intermediate hole and assumed no tensile strength in the formation (section 3.1.1). This gradient can be related to surface injection pressure by considering first that $P_f = P_s + P_h$, where P_f is the downhole fluid pressure, P_s is the surface injection pressure and P_h is the hydrostatic pressure. The hydrostatic pressure can be calculated by $P_h = 0.433\,\text{psi/ft} \times d \times SG$, where d is the depth of the injection interval in feet, SG is the specific gravity of the injectate (1.167 for pure brine), and 0.433 psi/ft is the assumed hydrostatic pressure gradient of the formation water. The pressure gradient is given by:

$$F_{gradient} = \frac{P_f}{d} = \frac{P_S + 0.433\,\text{psi/ft} \times SG \times d}{d} \; . \qquad (15)$$

Solving for surface injection pressure gives:

$$P_S = \left(\mathrm{F}_{gradient} - 0.433\,\mathrm{psi/ft} \times SG \right) \times d \ . \qquad (16)$$

Using 13,140 ft as the depth to the first main Paradox salt member (depth not corrected for borehole deviation), a pressure initiation gradient of 0.97 psi/ft, and a specific gravity of 1.167, EPA computed the corresponding surface injection pressure to be 6106 psi (Environmental Protection Agency, 1997). Because no friction loss in the tubing was included in the above computation, a surface injection pressure of 6106 psi is a conservative estimate of the surface pressure required to initiate fracturing in the confining layer (i.e., the actual value accounting for friction loss would be higher). Based on the above analyses, EPA originally placed the MASIP for the PVU injection well at 5000 psi (Environmental Protection Agency, 1997).

In 2004, the permitted MASIP was increased to 5350 psi. This value was based on the same 0.97 psi/ft fracture initiation gradient as when the 5000 psi MASIP was selected. A pressure of 6106 psi was still considered necessary to breach the confining salt, and therefore an injection pressure of 5350 psi was considered low enough to prevent a breach of the confining layer (Environmental Protection Agency, 2004). The emphasis in this analysis was the stress gradient (pressure gradient) applied at the base of the salt for a given surface injection pressure, as compared to the 0.97 psi/ft fracture initiation pressure gradient for the salt confining layer. With a surface injection pressure of 5350 psi, the stress gradient at the base of the salt was calculated to be 0.8977 psi/ft (using equation 16). Following the same procedure, we calculated the stress gradient at the base of the salt given an increase in the MASIP. Given an MASIP of 5500 psi, the stress gradient at the base of the salt is calculated to be 0.9108 psi/ft (Table 2), within ~6% of 0.97 psi/ft pressure initiation gradient. If the MASIP were raised to 5800 psi, the resulting gradient at the base of the salt would be 0.933 psi/ft, within ~ 4% of the calculated pressure initiation gradient in the salt.

Table 2 - Calculated stress gradients given different surface injection pressures, following the methodology in the 2004 EPA permit. Depths and formations correspond to those evaluated in the 2004 permit.

Formation	Depth of Formation Base (feet)	Stress Gradient at 5000-psi Surface Injection Pressure	Stress Gradient at 5350-psi Surface Injection Pressure	Stress Gradient at 5500-psi Surface Injection Pressure	Stress Gradient at 5800-psi Surface Injection Pressure
Top Perforation	14080	0.862 psi/ft	0.8866 psi/ft	0.8972 psi/ft	0.9185 psi/ft
Molas	14024	0.863 psi/ft	0.8887 psi/ft	0.8988 psi/ft	0.9202 psi/ft
Pinkerton Trail	13894	0.864 psi/ft	0.8891 psi/ft	0.8999 psi/ft	0.9214 psi/ft
Lower Paradox Carbonate	13731	0.870 psi/ft	0.8962 psi/ft	0.9072 psi/ft	0.9290 psi/ft
Salt	13606	0.874 psi/ft	0.8977 psi/ft	0.9108 psi/ft	0.9329 psi/ft

The fracture initiation pressure gradient of 0.97 psi/ft at the base of the salt was calculated from geophysical well logs and is only an estimate. This value was calculated from sonic logs using assumed density-velocity relationships (section 4.1). No error analysis has been performed for these calculations and therefore the uncertainty of the 0.97 psi/ft estimated value is unknown. Also, the plasticity of the salt was not taken into account in these calculations.

The analyses included in the EPA permits to determine the MASIP only considered the fracture initiation pressure in the salt, not the fracture closure pressure. However, if the plasticity of the salt causes the stress within this confining unit to be isotropic as discussed in the previous section, then the fracture closure pressure gradient within the salt is equal to the overburden pressure gradient of ~1.1 psi/ft (Dewan, 1988c), higher than the 0.97 psi/ft fracture initiation pressure gradient used in the permits. A recent consultant review board (CRB) convened by Reclamation to review these MASIP calculations agreed that the salt should be considered to have an isotropic/lithostatic stress state and suggested re-computing fracture closure pressures using the overburden pressures (vertical stresses) (Wang et al., 2015). Hence, the CRB considered the fracture gradient value of 0.97 psi/ft used in the original calculations to be unrealistically low for evaluating the confining ability of the salt and hence considered the current MASIP for PVU Injection Well #1 to be conservative (Wang et al., 2015).

3.4 Requirements to increase the MASIP

In the 2011 EPA reauthorization of the well (Environmental Protection Agency, 2011), the EPA allowed for the possibility to increase the MASIP subject to four analyses:

i. An analysis of the adequacy of the injection equipment, well head, and downhole tubulars to withstand the proposed maximum allowable surface injection pressure.
ii. An analysis of the potential for adverse seismic activity if injection pressures are increased.
iii. An analysis of the continued adequacy of the confining zones, including information on the potential vertical fracture growth in the confining layers as a result of an increase in injection pressure.
iv. A demonstration made by performing a step rate injection test, using fluid normally injected, to determine both the instantaneous shut-in pressure and the formation breakdown pressure.

An analysis of the adequacy of the injection equipment was previously performed in order to increase the MASIP to 5350 psi (Environmental Protection Agency, 2004). The details of the pressure ratings of specific parts of the injection system are detailed in the 2004 EPA permit. In addition, future seismicity rates were evaluated in terms of the excess energy from fluid injection as a function of time (Environmental Protection Agency, 2004), although those analyses have since been superceded by more recent work. A detailed, up-to-date look at the seismic history of the PVU and its relationship to injection operations is provided in subsequent sections.

4 Induced Seismicity

Seismicity has been induced in the vicinity of the PVU injection well since the initial injection tests. Although the majority of the seismicity has been of small magnitude, several dozen felt events have occurred, including three earthquakes with M_L of 4.0 or greater. A major concern for increasing the MASIP is the potential for PVU to induce large-magnitude events more frequently, for the maximum magnitude of induced earthquakes to increase, or for the induced seismicity to migrate closer to populated areas. Below we review the lateral and vertical expansion of the induced seismicity, including an examination of the seismicity very close to the well and what it suggests about the effectiveness of the confining layer. We then evaluate how an increase in the MASIP might influence future induced seismicity, based on previous analyses of the seismicity data and its relation to injection parameters.

4.1 Plan View Evolution of Induced Seismicity

More than 6,000 shallow earthquakes (locating less than 8.5 km (27,900 ft) deep with respect to the ground surface elevation at PVU Injection Well #1) have been recorded in the vicinity of Paradox Valley since PVU injection operations began in 1991 (Block et al., 2015a). No such shallow earthquakes were detected in six years of seismic monitoring prior to the start of injection operations. Earthquakes were first detected 4 days after the start of the initial injection test into PVU Injection Well #1 in July, 1991 (Block et al., 2014; Block et al., 2015a). The first earthquakes occurred very close to the injection well. As injection continued, earthquakes continued to occur close to the well but also began occurring at increasing distances from the well. At present, earthquakes have occurred up to ~18 km from the injection well (Figure 9).

The geographical distribution of induced seismicity over time is illustrated in the series of maps from Wood et al. (2015), presented in Figure 10 and Figure 11. The rate of geographical expansion of seismicity has varied over time, but generally the maximum distance of induced earthquakes from the well has increased. The rate of expansion was highest during the later injection tests (1991-1995) and the early phase of continuous injection (1996-2000) (Figure 10). In mid-2000, when the PVU injection flow rate was decreased by about 33% in response to a M_L 4.3 induced earthquake, the geographical expansion of seismicity slowed, and the spatial extent of the near-well area (< ~5 km from well) and Northwest (NW) seismicity cluster (6-8 km NW of well) largely stabilized (Wood et al., 2015). While new clusters of seismicity appeared along the edges of northern Paradox Valley in the years following the reduction in flow rate, seismicity rates there were very low (Wood et al., 2015).

This relatively stable period lasted until 2009. Five induced earthquakes of magnitude 2.5 or greater occurred in 2009. This was the highest annual rate of M 2.5+ earthquakes in five years, and the second highest rate since the injection flow rate was reduced in mid-2000 (Wood et al., 2015). A distinct group of earthquakes developed in 2010 about 6 km southeast of the injection well, the southeast (SE) cluster. While the first detected SE-cluster event occurred in 2004, with

two additional events recorded in 2008 and 2009, beginning in 2010 the SE cluster experienced increasing rates of seismicity (Wood et al., 2015).

Seismicity rates within the northern-valley area have also changed in recent years. During each year from 2000 (when the northern valley seismicity was first detected) to 2009, between two and 33 earthquakes were recorded. In 2010, the rate increased markedly: 557 northern-valley earthquakes were recorded, with the majority occurring in a single swarm lasting just 16 days (Block and Wood, 2011). Northern-valley seismicity rates remained elevated during 2011, with 113 earthquakes recorded (Block and Wood, 2012), but declined back to pre-2010 rates during 2012, with just 10 events recorded (Block and Wood, 2013).

Beginning in mid-2010, several shallow earthquakes have been detected beneath the floor of Paradox Valley. Three earthquakes were detected in 2010; two in 2011; five in 2012, five in 2013, and four in 2014 (Block et al., 2015a). No earthquakes were detected beneath Paradox Valley in the 25 years of seismic monitoring prior to 2010 (Block and Wood, 2011). If the maximum magnitude of these earthquakes were to increase substantially, they would be of particular concern due to the fact that some of them are as close as ~1.7 km to the town of Paradox (Figure 11). However, the largest of the earthquakes that has occurred to date beneath Paradox Valley has a duration magnitude of 1.4, which is well below the magnitude threshold for human detection of ~M 2.5.

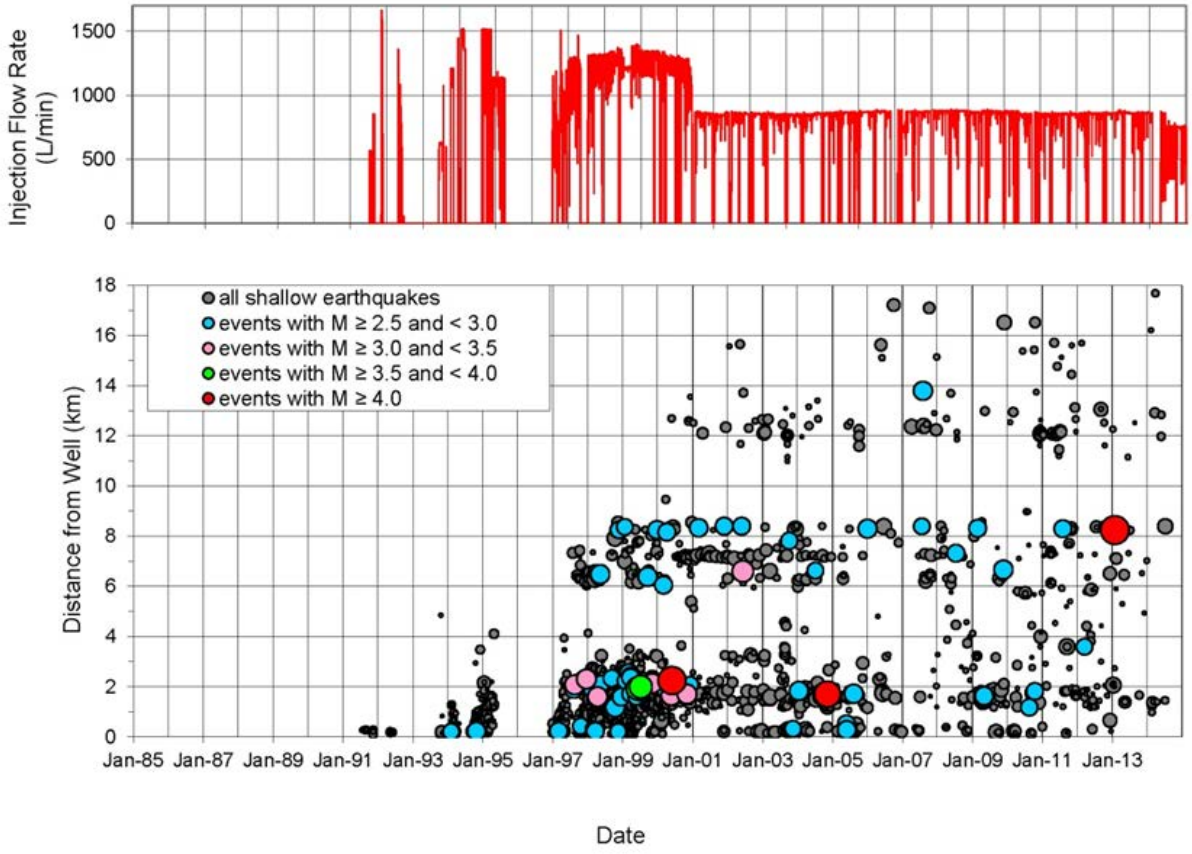

Figure 9 – From Block et al. (2015a). (Top) Daily average injection flow rate. (Bottom) Scatter plot of earthquakes with M ≥ 0.5 and depth < 8.5 km (relative to the ground surface elevation at the injection wellhead), plotted as a function of date and distance from PVU Injection Well #1. Each circle represents a single earthquake, with the width of the circle scaled by the event magnitude.

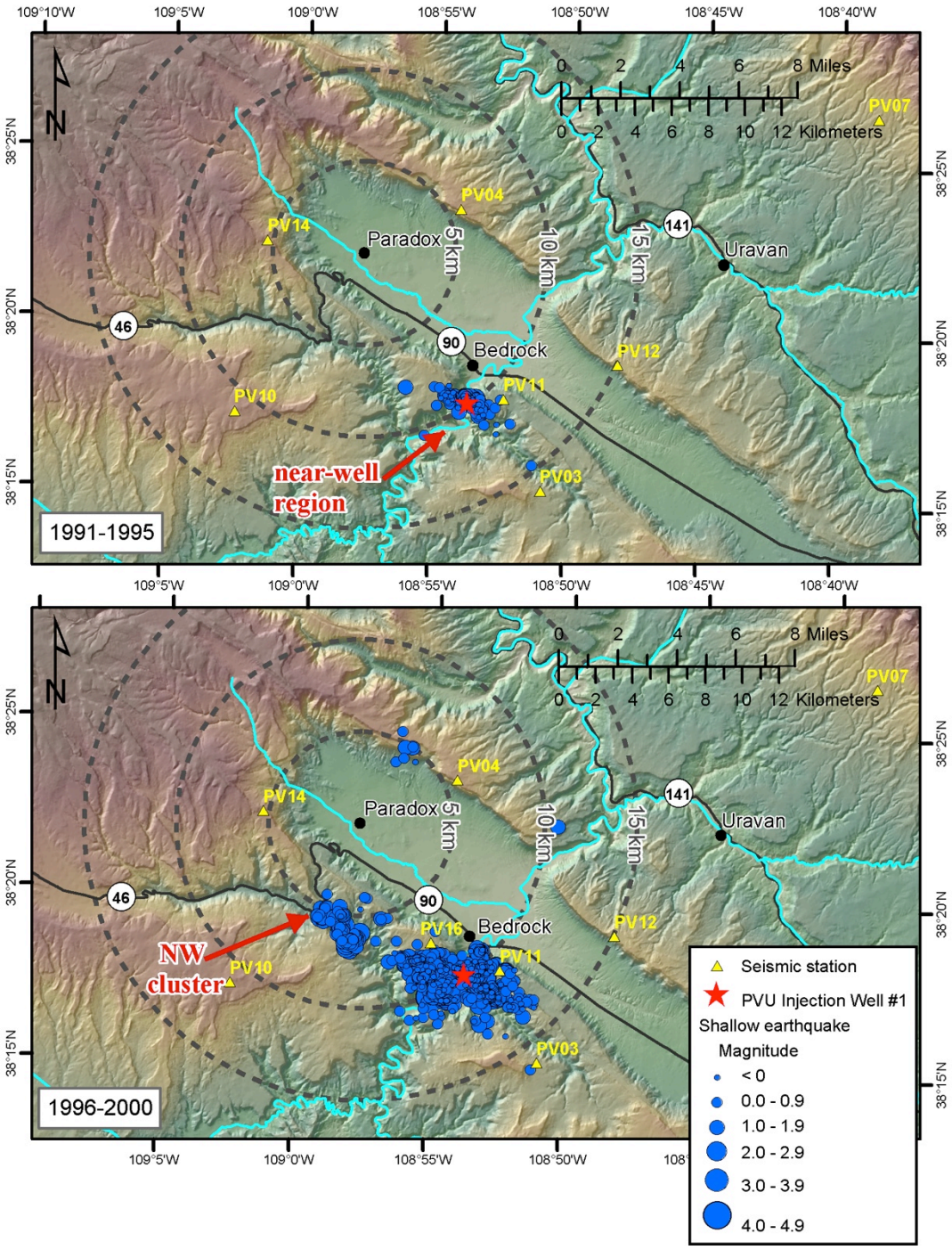

Figure 10 – From Wood et al. (2015). Maps showing the geographical distribution of shallow seismicity recorded in the Paradox Valley area from 1991 through 2000: (top) injection tests, 1991-1995 (bottom) long-term injection, 1996-2000. All detected earthquakes less than 8.5 km deep (relative to the ground surface elevation at the injection wellhead) are included. Dashed circles show distance from the town of Paradox.

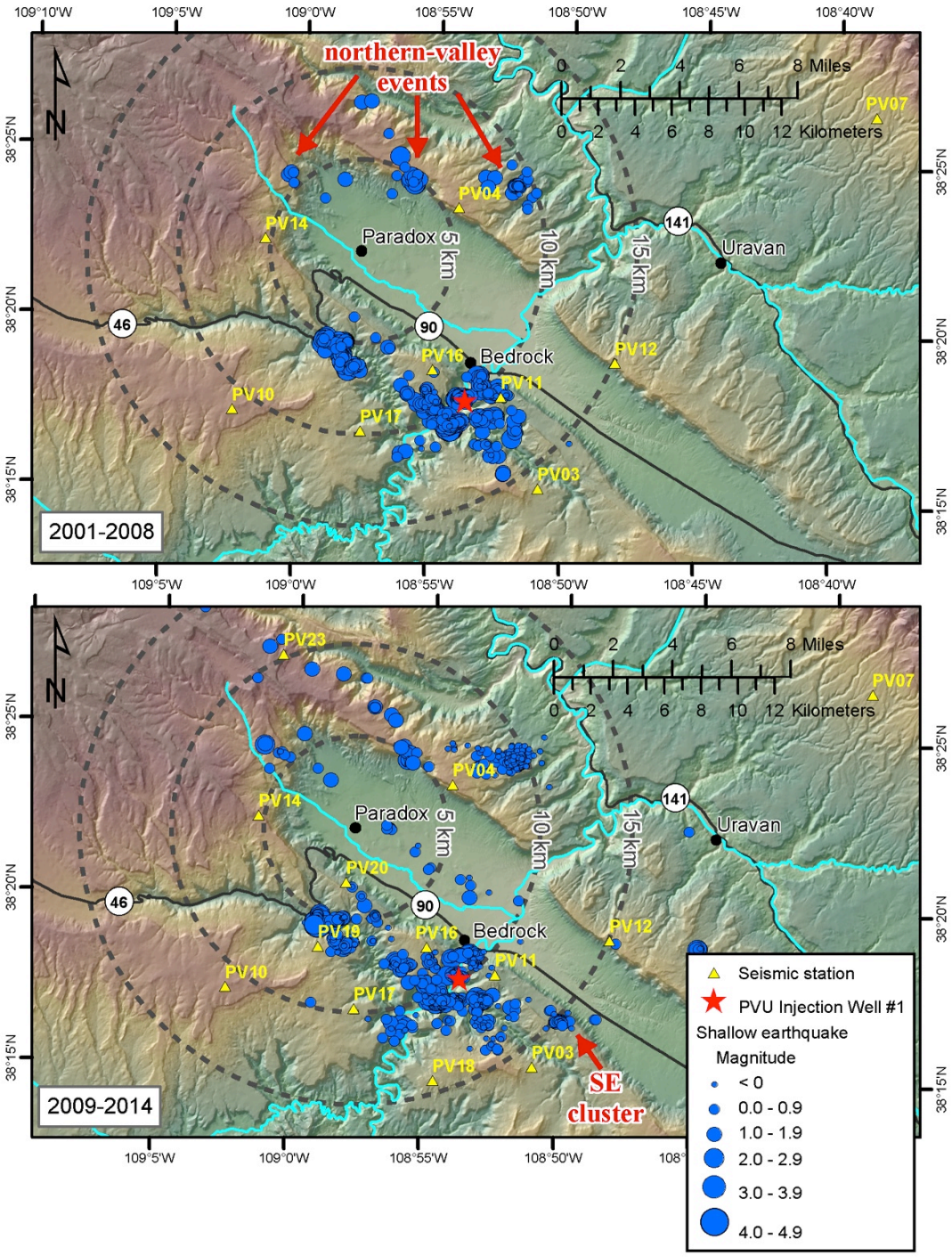

Figure 11 - From Wood et al. (2015). Maps showing the geographical distribution of shallow seismicity recorded in the Paradox Valley area from 2001 through 2014: (top) long-term injection, 2001-2008 (bottom) long-term injection, 2009-2014. All detected earthquakes less than 8.5 km deep (relative to the ground surface elevation at the injection wellhead) are included. Dashed circles show distance from the town of Paradox.

4.2 Vertical Extent of Induced Earthquakes

Although the injection interval is relatively narrow in the PVU wellbore, induced earthquakes near the well span a depth range exceeding 2 km (Figure 12). As the structure of the subsurface is poorly constrained, it is not definitively known in which formations earthquakes are occurring. Block et al. (2015b) mapped subsurface geology and faults using relatively-relocated hypocenters (Figure 12). This analysis relied on the assumption that the majority of earthquakes occur within or near the Leadville formation. The presence of normal faults was inferred by abrupt lateral offsets in earthquake depths (Figure 12).

The depth range of earthquakes closest to the injection well, where pore pressures are expected to be the highest, can be used to evaluate the effectiveness of the confining layer. Earthquakes within a few hundred meters of the well span a depth range of roughly 500 m (Figure 13 to Figure 16). The depths of these earthquakes appear to correspond approximately to the base of the Leadville formation to just above the top of the Paradox salt formation, based on the known formation depths in the PVU wellbore and assuming horizontal layers. If the formations are not vertically offset by faults, then many of these earthquakes appear to be occurring at depths shallower than the base of the confining Paradox Salt formation (~ -2.65 km below sea level at the well) (Figure 13 to Figure 16). The shallowest earthquake having a robust relatively-relocated hypocenter occurs at an elevation of -2.27 km, above the top of the Paradox Salt confining layer at the well. While the errors in relative earthquake locations are small (< ~50 m), absolute locations likely have larger errors (>100 meters) and can shift a few hundred meters depending on the velocity model used. Therefore, there is relatively large uncertainty in the absolute hypocenters of these earthquakes that complicates direct comparison with the known stratigraphy at the well.

Possible interpretations of these shallow earthquakes include:

- The Paradox Salt has not acted as an adequate confining layer.
- There are structures (faults) in the immediate vicinity of the well that vertically offset reservoir formations.
- Shallow earthquake depths are the result of absolute earthquake location errors.
- These earthquakes are triggered by mechanisms different than pore-pressure alteration.

The shallow earthquakes began in May 1992 during injection testing, when pressures at the well were relatively low (3694 psi surface pressure, 10,539 psi down-hole pressure; Figure 4). Cross sections through these events over time show that the shallower events began during the same time period as the deeper events, and that the events initially occurred within two depth intervals separated by an aseismic zone (Figure 14 and Figure 16). While the shallow (> -2.65 km elevation) earthquakes occurred throughout injection testing and long-term injection, they have not substantially expanded vertically or horizontally since 1993-1994 (Figure 14 and Figure 16). These observations suggest that the shallow earthquakes are not related to vertical fracturing through the Paradox Salt formation. If the confining layer had been breached, the breach would likely have occurred when injection pressures were high, the hypocenters of the early events would likely have migrated from greater depths to shallower depths over time, and earthquakes

would likely have continued to expand vertically and laterally at shallow depths during long-term injection.

Most of the shallow events near the well occur on or near a single northeast-trending epicenter lineation. In addition, many deeper events occur immediately north of this lineation, while few earthquakes occur immediately south of it (Figure 12). This epicenter pattern suggests that the shallow events may be occurring on a fault that vertically offsets target injection formations. In addition, the azimuths of both the fault planes inferred from earthquake focal mechanisms and epicenter lineations of the shallow events are different from those of the nearby deeper events (Figure 17), further suggesting a structural explanation for the occurrence of the shallow events.

In reference to the vertical extent of earthquakes near the PVU injection well, a consultant review board convened by Reclamation in January, 2015, suggested an analysis of the waveforms of the shallower and deeper events (Wang et al., 2015). The presence of a discrete subsurface salt layer can result in distinct secondary seismic phases due to reflection and phase conversion off of the salt formation (e.g., Kraaijpoel and Dost, 2013). Preliminary examination of earthquake waveforms does not show easily recognizable secondary phases (Figure 18). It is expected that these secondary phases would move out as a function of earthquake depth. Thus far, no such secondary phases have been observed. This preliminary examination has been performed on multiple distinct coeval earthquake clusters. These observations suggest that there is not a distinct seismic discontinuity which separates these earthquakes spanning a range of depths. Still, a detailed analysis, possibly incorporating waveform modeling, may better resolve the depths of these earthquakes relative to the geologic structure.

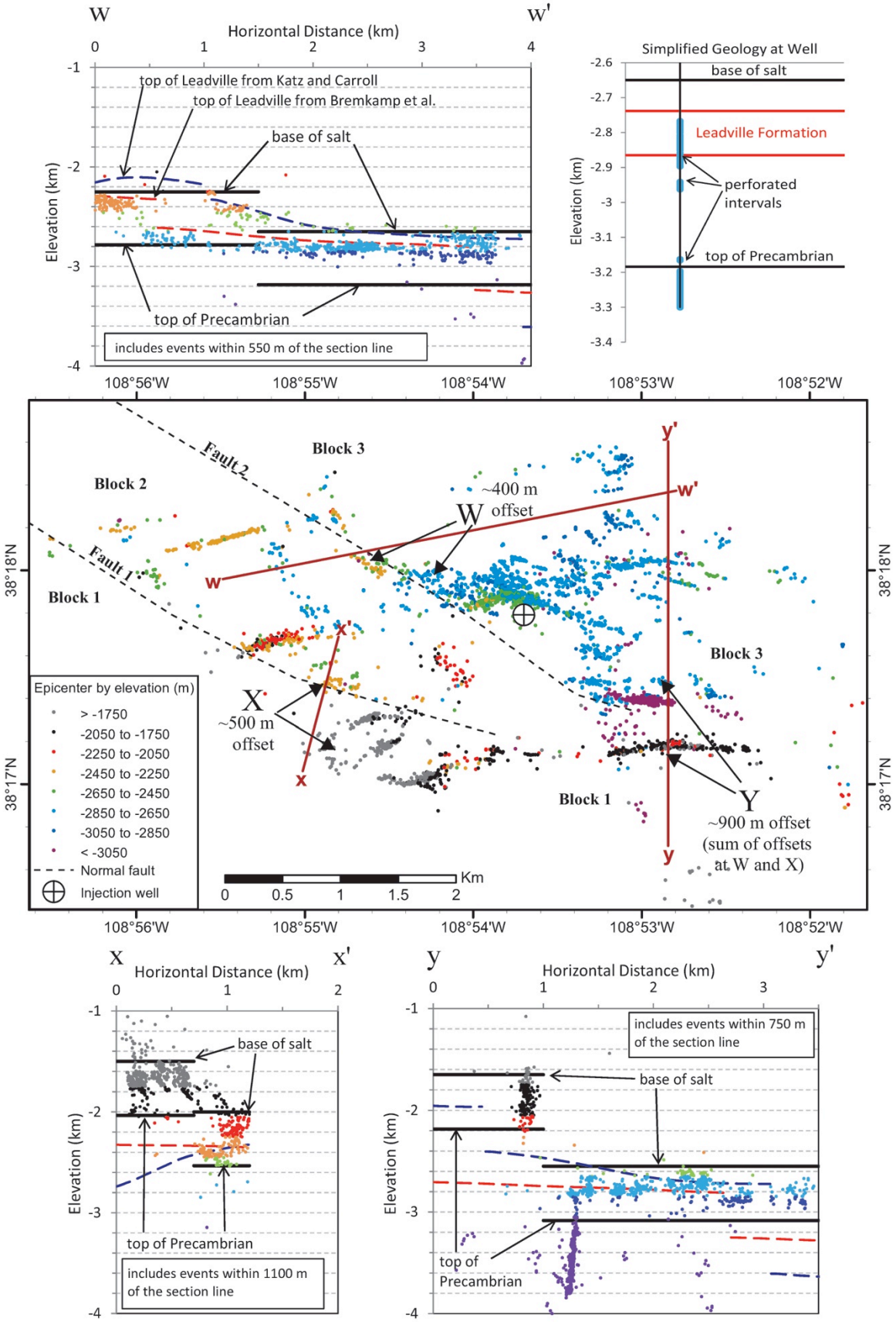
W
W'
Horizontal Distance (km)
top of Leadville from Katz and Carroll
top of Leadville from Bremkamp et al.
base of salt
top of Precambrian
includes events within 550 m of the section line
Elevation (km)
Simplified Geology at Well
base of salt
Leadville Formation
perforated intervals
top of Precambrian
Block 1
Block 2
Block 3
Fault 1
Fault 2
~400 m offset
~500 m offset
~900 m offset (sum of offsets at W and X)
Epicenter by elevation (m)
> -1750
-2050 to -1750
-2250 to -2050
-2450 to -2250
-2650 to -2450
-2850 to -2650
-3050 to -2850
< -3050
Normal fault
Injection well
Km
108°56'W
108°55'W
108°54'W
108°53'W
108°52'W
38°18'N
38°17'N
x
x'
y
y'
includes events within 1100 m of the section line
includes events within 750 m of the section line

Figure 12 – Previous Page. From Block et al. (2015b). Map showing epicenters of earthquakes occurring in the near-well region of induced seismicity, color-coded by hypocenter elevation (center), and cross sections showing distinct vertical offsets of hypocenters (top and bottom). Only a-quality hypocenters from the event relative location are included. The labels 'W', 'X', and 'Y' on the map identify abrupt lateral changes in hypocenter elevations. Two northwest-striking normal faults interpreted from the hypocenter elevation patterns are shown. Our interpreted base of the Paradox salt and top of the Precambrian (solid black lines) and the interpreted top of the Leadville formation from Katz and Carroll (1984) (dashed blue line) and Bremkamp et al. (1984) (dashed red line) are shown in each cross section. A simplified geologic section at the PVU wellbore is included at upper right for reference. Note the color-scale used in this plot and those in Block et al. (2015b) are distinct from those in the following figures.

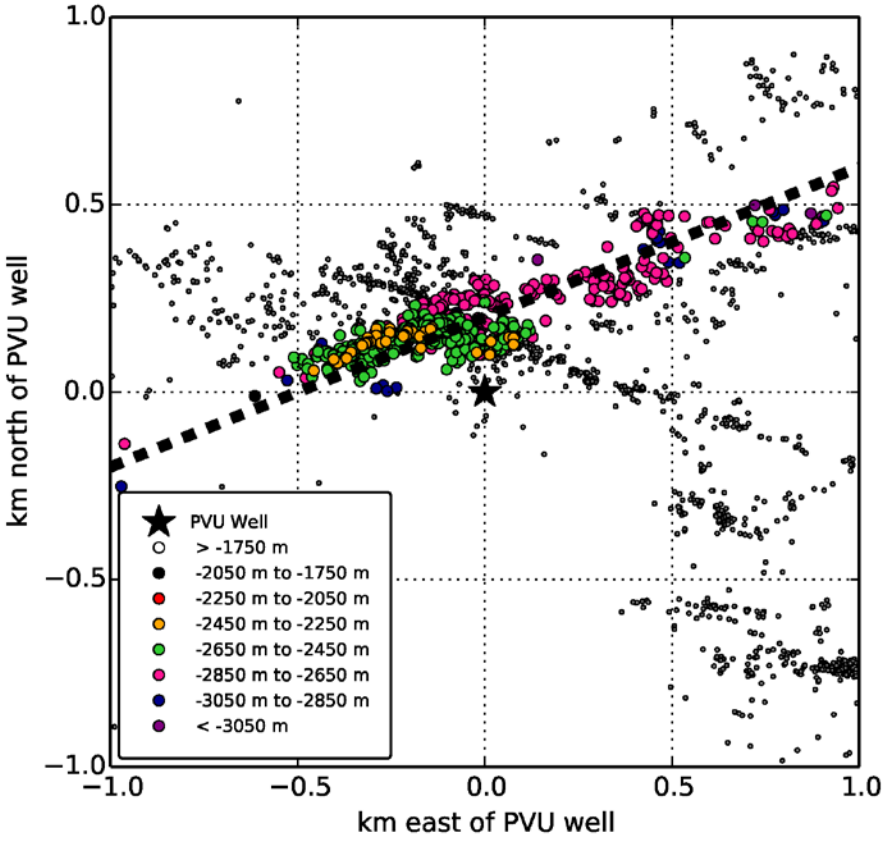

Figure 13 - Map of earthquakes near the PVU injection well. Earthquakes within 0.1 km of the transect (black dashed line) are selected and colored by elevation (see legend). The temporal evolution of depth sections along this transect are shown in Figure 14.

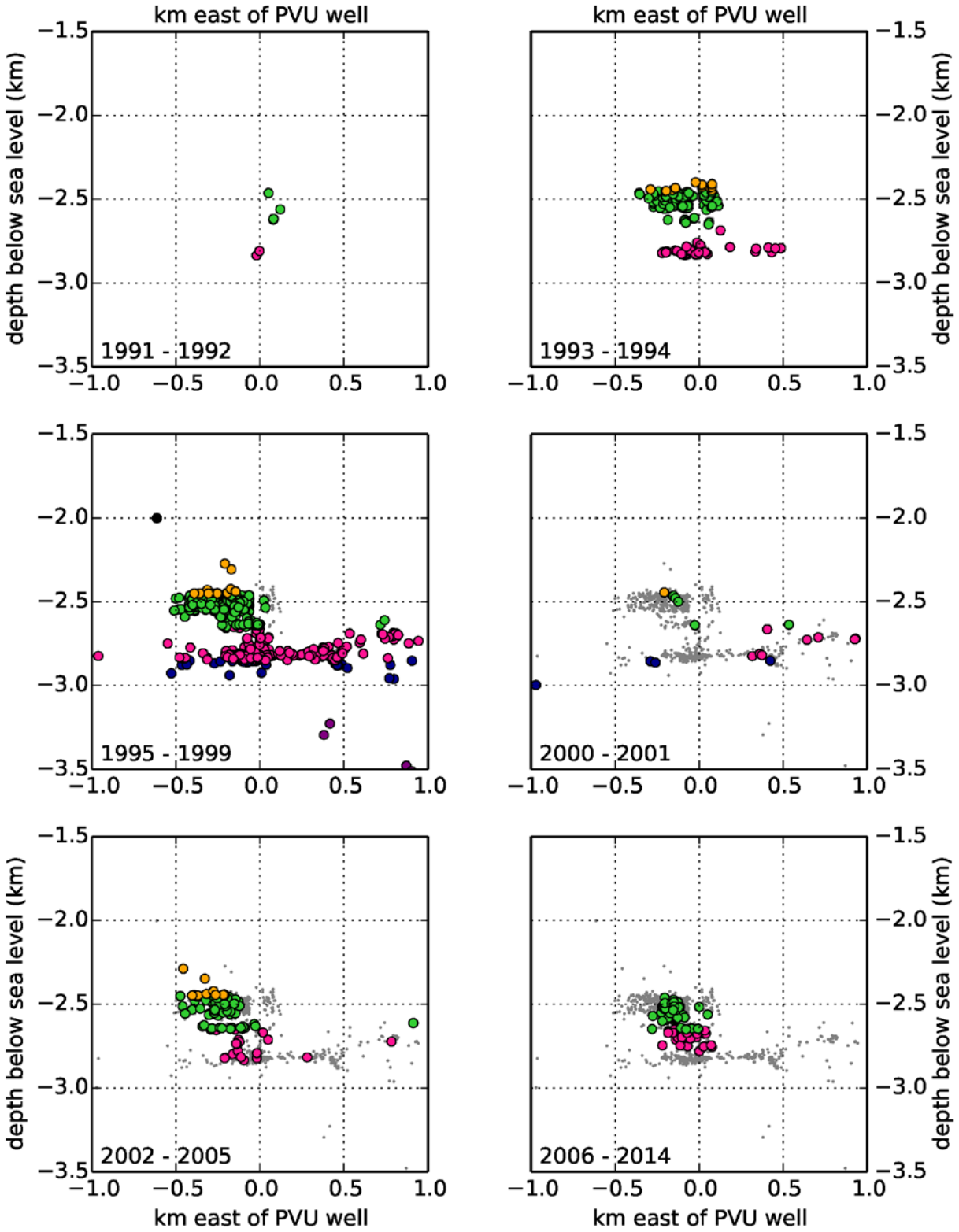

Figure 14 – Time and depth evolution of earthquakes from the cross section delineated in Figure 13. Earthquakes are colored by elevation (depth), as in Figure 13. All earthquakes previous to each time window are shown as gray dots.

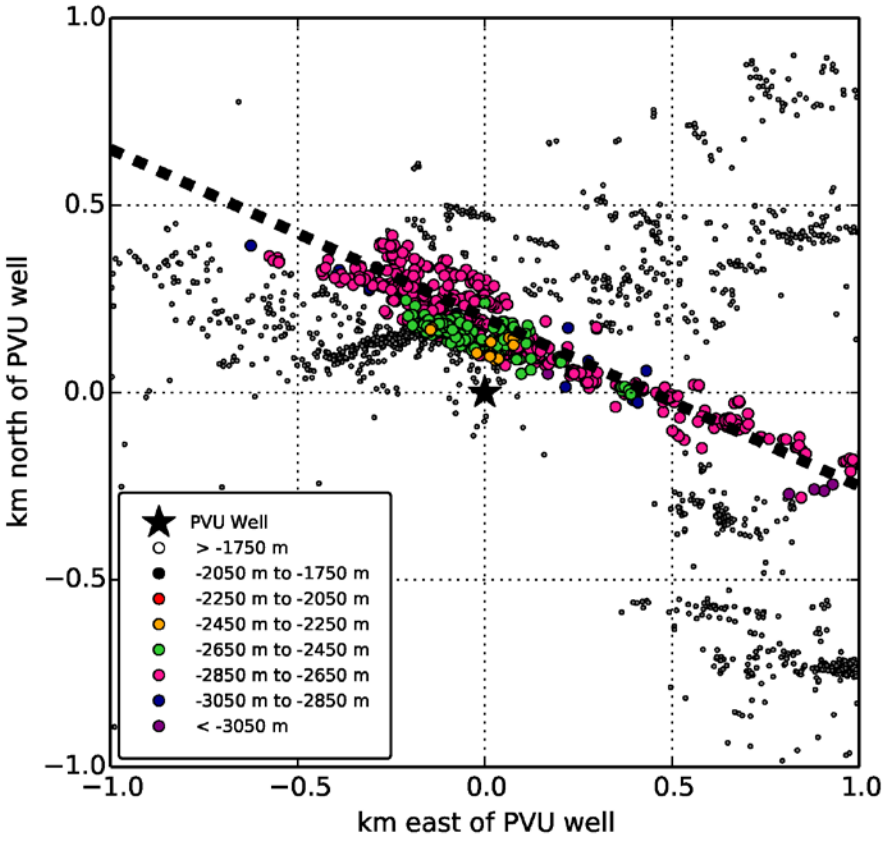

Figure 15 - Map of earthquakes near the PVU injection well. Earthquakes within 0.1 km of the transect (black dashed line) are selected and colored by elevation (see legend). The temporal evolution of depth sections along this transect are shown in Figure 16.

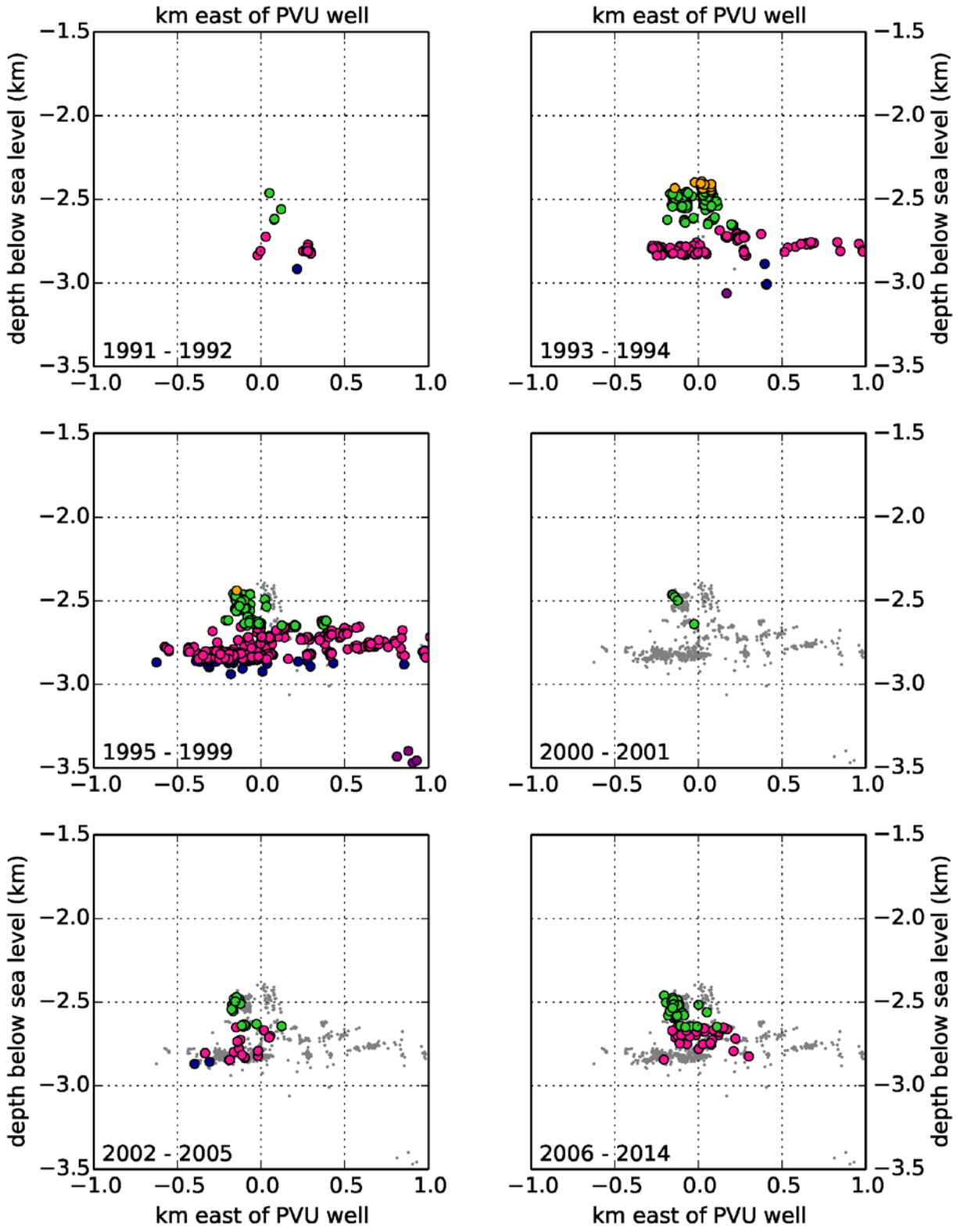

Figure 16 - Time and depth evolution of earthquakes from cross section delineated in Figure 15. Earthquakes are colored by elevation (depth), as in Figure 15. All earthquakes previous to each time window are shown as gray dots.

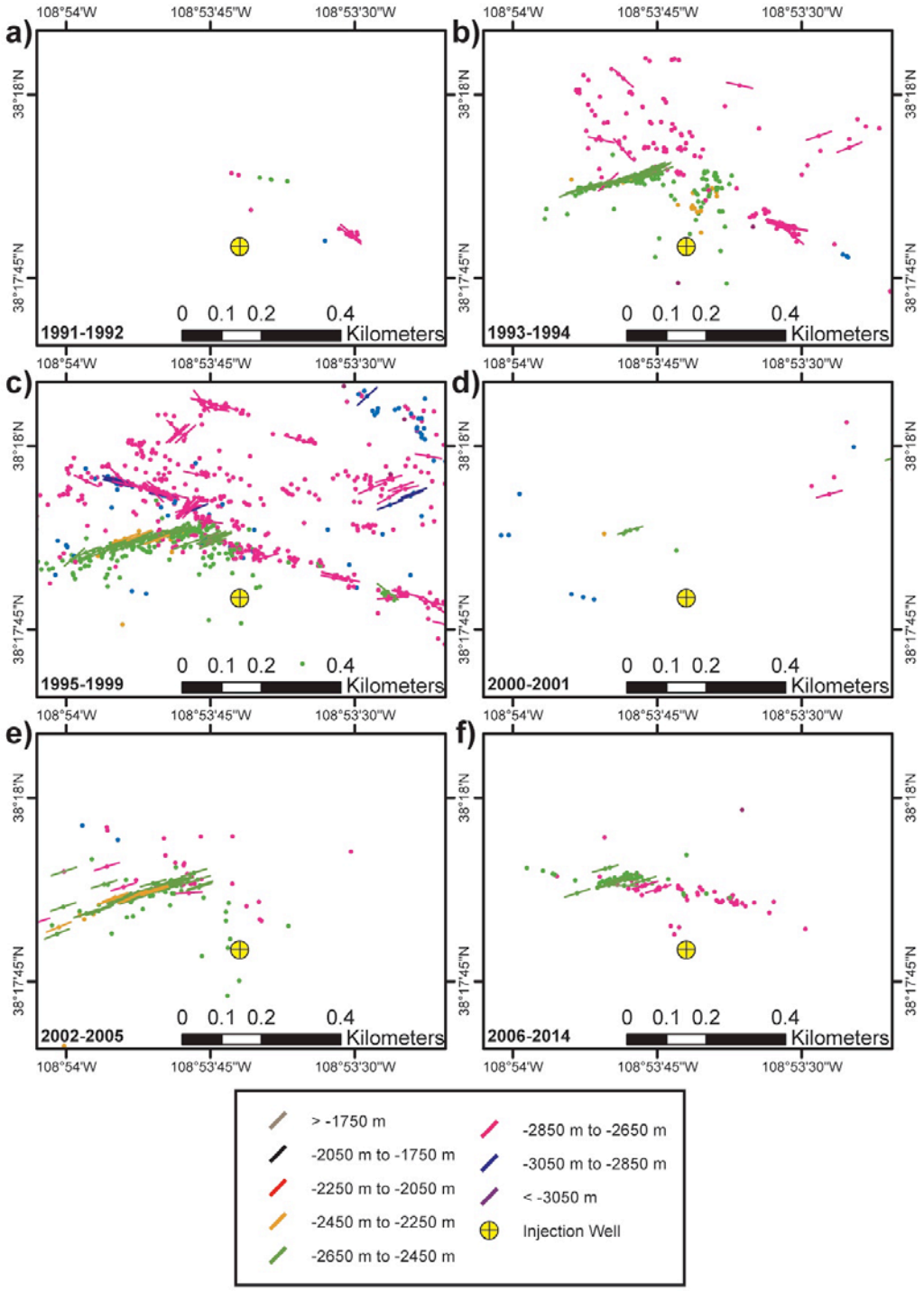

Figure 17 - Time and depth evolution of focal mechanisms. Time windows include: (a) 1991–1992; (b) 1993–1994; (c) 1995–1999; (d) 2000–2001; (e) 2002–2005; (f) 2006–2014. The strike of the preferred fault plane is shown as a solid line, colored by elevation (see legend). (See Block et al. (2015b) for details of the focal mechanism analysis.)

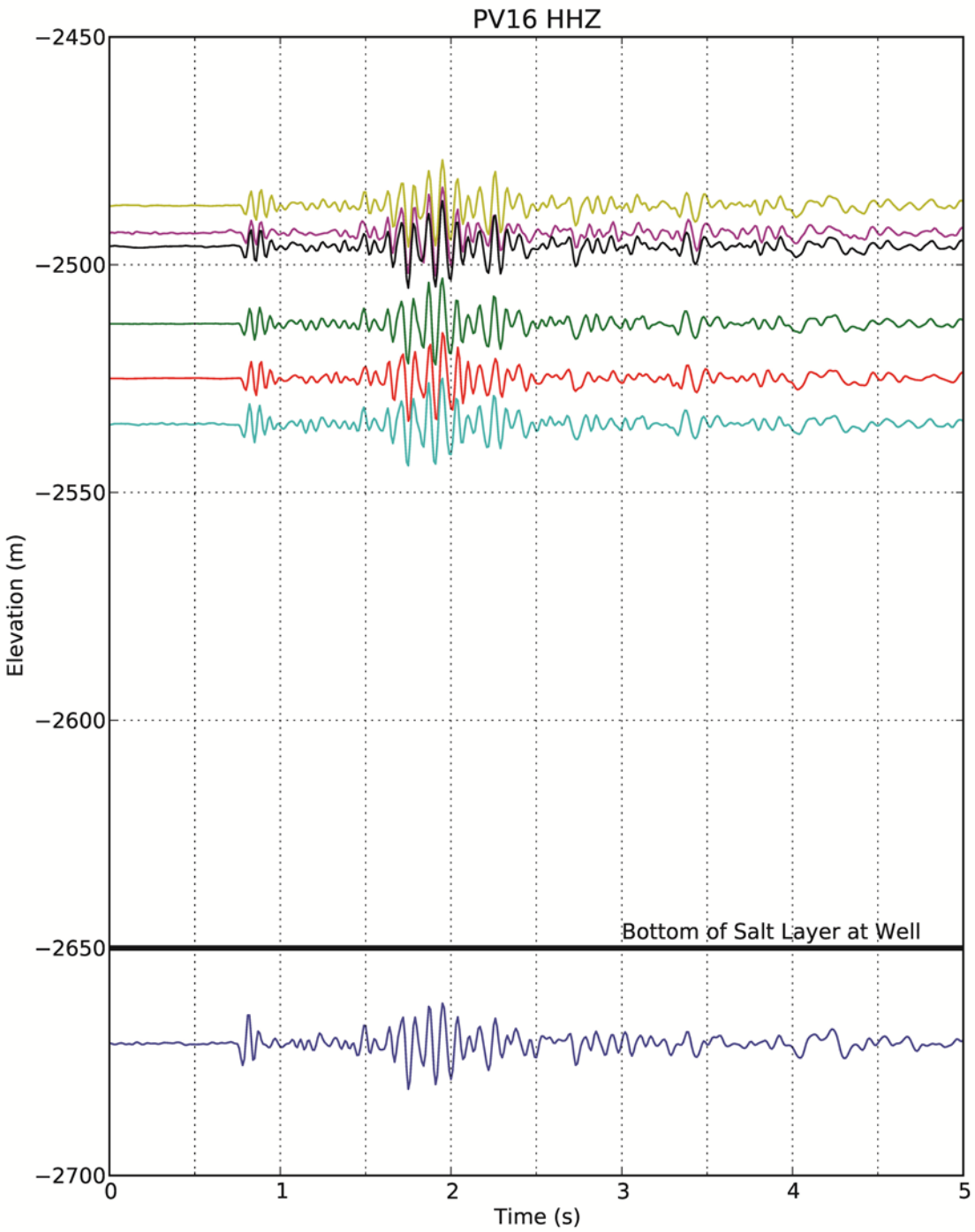

Figure 18 – Earthquake waveforms recorded on the vertical component at station PV16. These earthquakes occur in a small cluster and span a range of depths. The black line denotes the bottom of the salt formation at the well. If the salt layer were also at this depth at the location of this seismicity cluster, we would expect to see secondary phases on the waveforms related to reflection of seismic energy off the salt interface. While there is some change in the P-S time between events, there are no distinct arrivals which could be attributed to secondary phases (e.g., reflections off the salt formation).

4.3 Effects of Increasing the MASIP

Injection parameters can have substantial impact on the characteristics of seismicity induced near an injection well. Empirical correlations reviewed in this section suggest that both the rates and magnitudes of events occurring within ~5 km of the PVU well are influenced by temporal variations in average injection pressure. The increase in maximum earthquake magnitude over time correlates both with cumulative injected fluid volume and with the spatial expansion of seismicity clusters, which in turn are related to the injection flow rate and the propagation of pore pressure perturbations introduced at the injection well. At PVU, injection parameters have been altered several times in an effort to reduce the occurrence of large-magnitude earthquakes. Reduction in flow rate and increased injection well shut-in time following large-magnitude earthquakes in 1999-2000 and 2013 resulted in substantially decreased seismicity rates (Block and Wood, 2009; Block et al., 2015a). Based on the relation between injection parameters and induced seismicity observed to date, substantial increases in average injection flow rates and/or injection pressures, such as might occur in association with an increase in the MASIP, are likely to have a noticeable adverse impact on future induced seismicity. Below we briefly review the relation between injection parameters and induced seismicity observed at PVU.

4.3.1 Induced Seismicity and its Relation to Pore Pressure

Block and Wood (2009) compared seismicity rates and magnitudes with four injection parameters: injectate volume, injection flow rate, down-hole pressure, and percent injection time. Down-hole pressure exhibited the best correlation with seismicity occurring within 5 km of the well. During early injection operations (1996 – 2000), seismicity rates and magnitudes correlate well with short-term ($\leq$ 6-month) averages of down-hole pressure. In contrast, later operations correlate with long-term (18-month to 30-month) averages of down-hole pressure (Figure 19). Higher average pressures correlate with increased seismicity rates and the occurrence of earthquakes with $M \geq 2.5$. Block and Wood (2009) did not observe similar correlations with seismicity in the Northwest Cluster, possibly because of the greater time required for pore pressure changes to propagate to greater distances and the decreased amplitude of the pressure perturbation with distance.

Even though a correlation between rates and magnitudes of distant induced seismicity and down-hole pressure is not apparent, it is likely that far-field reservoir pressurization is occurring (King and Block, 2015). This is supported by the fact that induced earthquakes have been occurring at greater distances over the lifetime of the well (Figure 10 and Figure 11). The renewed spatial expansion of the induced seismicity observed from 2009-2012 (Figure 11) correlates with increasing average injection pressures during this time period (Figure 19). Of particular note is the January 2013 M_L 4.4 earthquake that occurred 8.2 km northwest of the injection well. This earthquake was the first large ($> M_L$ 4) earthquake occurring outside of the near-well region (Block et al., 2014). In addition, recent analysis indicates that the initial onset of induced seismicity as a function of distance from the well is consistent with a model of simple 1-D pore

pressure diffusion (Figure 20), suggesting that pore pressure increase plays a major role in triggering of seismicity induced by PVU injection.

Given the relation between injection/pore pressure and induced seismicity discussed above, increased average injection pressures would be expected to lead to increased seismicity rates and increased likelihood of events with $M \geq 2.5$. In addition, seismicity may expand into previously-aseismic areas if these areas experience pore pressure increases sufficient to cause slip on preexisting fractures. These effects are related to local pore pressures, which respond to injection pressures applied at the well over substantial periods of time (months to years). Therefore, increased injection pressures that are only sustained for short periods of time (days to weeks), and are balanced by extra injection well shut-in time (such as might occur during short-term reservoir stimulation) would not be expected to substantially affect the induced seismicity, expect that occurring very close to the well.

4.3.2 Maximum Earthquake Magnitude

Following the January 2013 M_L 4.4 earthquake, Reclamation performed a detailed analysis of the estimated maximum earthquake magnitudes that PVU injection could induce (Yeck et al., 2015). The analysis was performed following two distinct methodologies. First, observed maximum magnitude earthquakes were compared to the cumulative injected volume of brine (Figure 21). This work shows that the logarithm of the cumulative injected volume is linearly related to the observed maximum magnitude earthquake. The second methodology relies on the size of individual clusters of earthquakes (Figure 22). Under the assumption that earthquakes delineate areas of pore-pressure alteration sufficient to cause shear slip and that earthquake rupture must remain confined within these clusters, estimated magnitudes were calculated based on the maximum fault size that could be contained in each cluster. This analysis shows that the rapid expansion early in the history of each cluster agrees well with the trend of observed maximum magnitudes over time. The results also indicate that there can be delays of several years between the time a cluster reaches a threshold for a given magnitude and the occurrence of such an event. Both analyses indicate that the estimated maximum earthquake magnitude increased rapidly during early injection operations and has remained fairly constant since about 2000.

Changes in injection operations in response to a higher MASIP could influence the rate of increase of maximum earthquake magnitude. This effect is likely to be minor, except possibly for events occurring within small earthquake clusters. If injection flow rates were increased, the cumulative injected fluid volume would increase at a faster rate, and therefore maximum earthquake magnitudes predicted with the cumulative volume model would also increase at a faster rate. However, since the increase in predicted earthquake magnitude is related to the logarithm of the cumulative injected volume, the absolute increase in estimated maximum earthquake magnitude would still be small. Maximum earthquake magnitudes predicted by the cluster model would only increase if pressure perturbations large enough to cause shear slip expand to larger areas – i.e., the seismicity clusters grow in size. The sizes of the near-well cluster and NW cluster have remained fairly constant since 2000, despite the increased average injection pressures during 2009-2012. Stratigraphy and faulting may be limiting their potential for growth. Because the rate of maximum magnitude increase is greatest when a seismicity cluster is small, maximum magnitude estimations for small clusters would be affected by an increase in cluster size much more than the larger seismicity clusters. Hence, it seems that the

only substantial change in maximum earthquake magnitude in response to increasing the MASIP would occur if currently-small seismicity clusters experience spatial expansion from increasing pore pressures. If increased injection pressures are sustained for long periods of time (months to years), then earthquake magnitudes in small seismicity clusters distant from the well (such as those in the northern Paradox Valley area) could increase. Because of the long time delays for pore pressure propagation to these areas, this potential increase in cluster size and maximum earthquake magnitude may not be observed for several years.

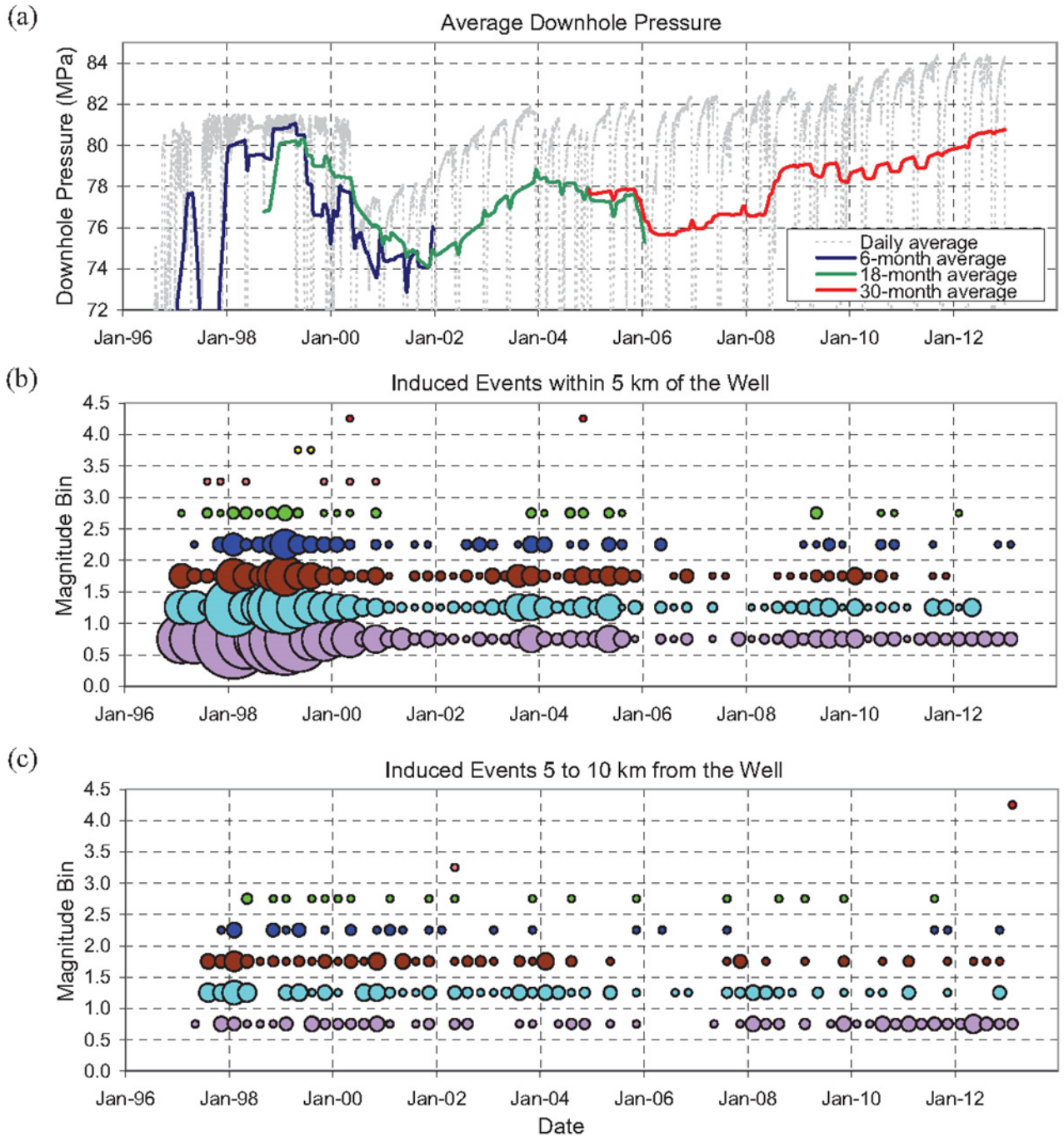

Figure 19 - from Block et al. (2014) (a) Injection downhole pressure data averaged over daily, 6-month, 18-month, and 30-month time periods, (b) occurrence of induced seismicity as a function of time and magnitude within 5 km of the injection well, and (c) at distances of 5–10 km from the well. In the seismicity plots, the area of each circle is scaled by the number of events in a given quarter-year and magnitude range. The low seismicity rate in the smaller magnitude bins from mid-2005 to mid-2007 in the bottom plot is believed to be due to an unusually large number of offline stations.

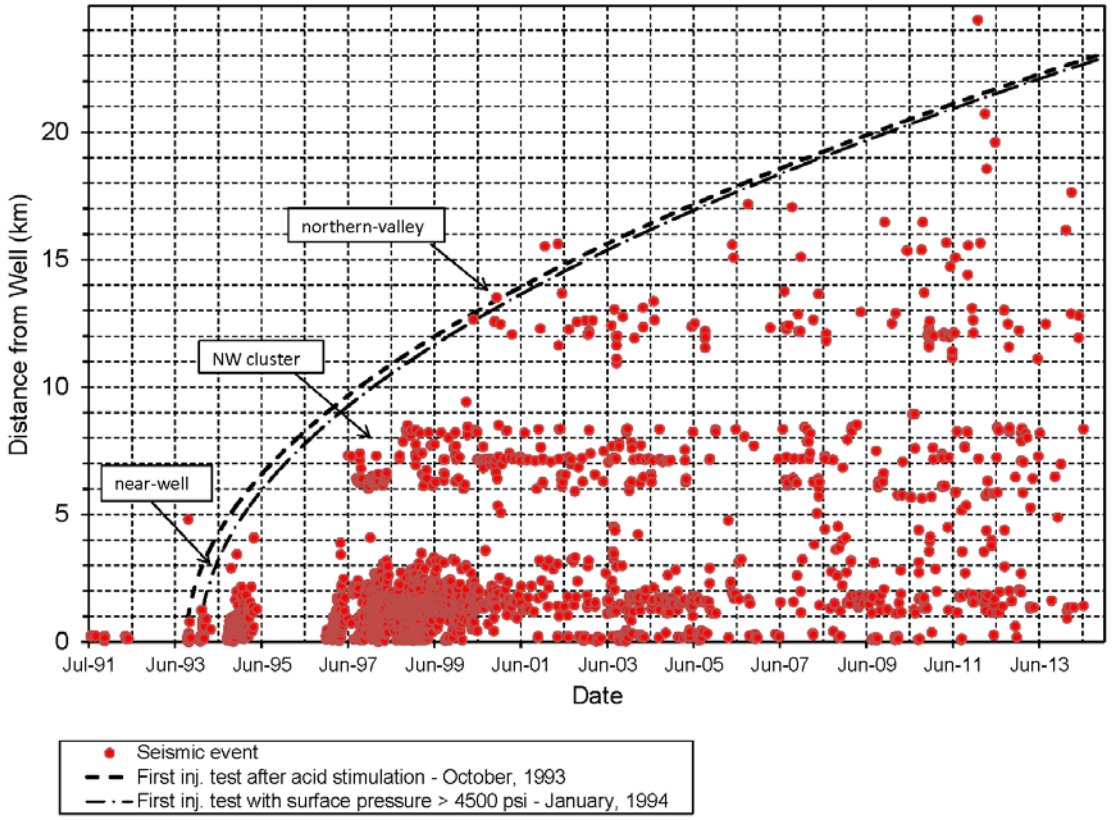

Figure 20 – from King and Block (2015). Seismicity time-distance plots of all shallow (depth < 8.5 km) events with magnitude ≥ 0.5 occurring in the vicinity of the PVU injection well. Seismic triggering fronts for the first two significant injection tests are overlaid. The triggering fronts were computed using a 1-D linear pressure diffusion model and a hydraulic diffusivity of 0.20 m^2/s.

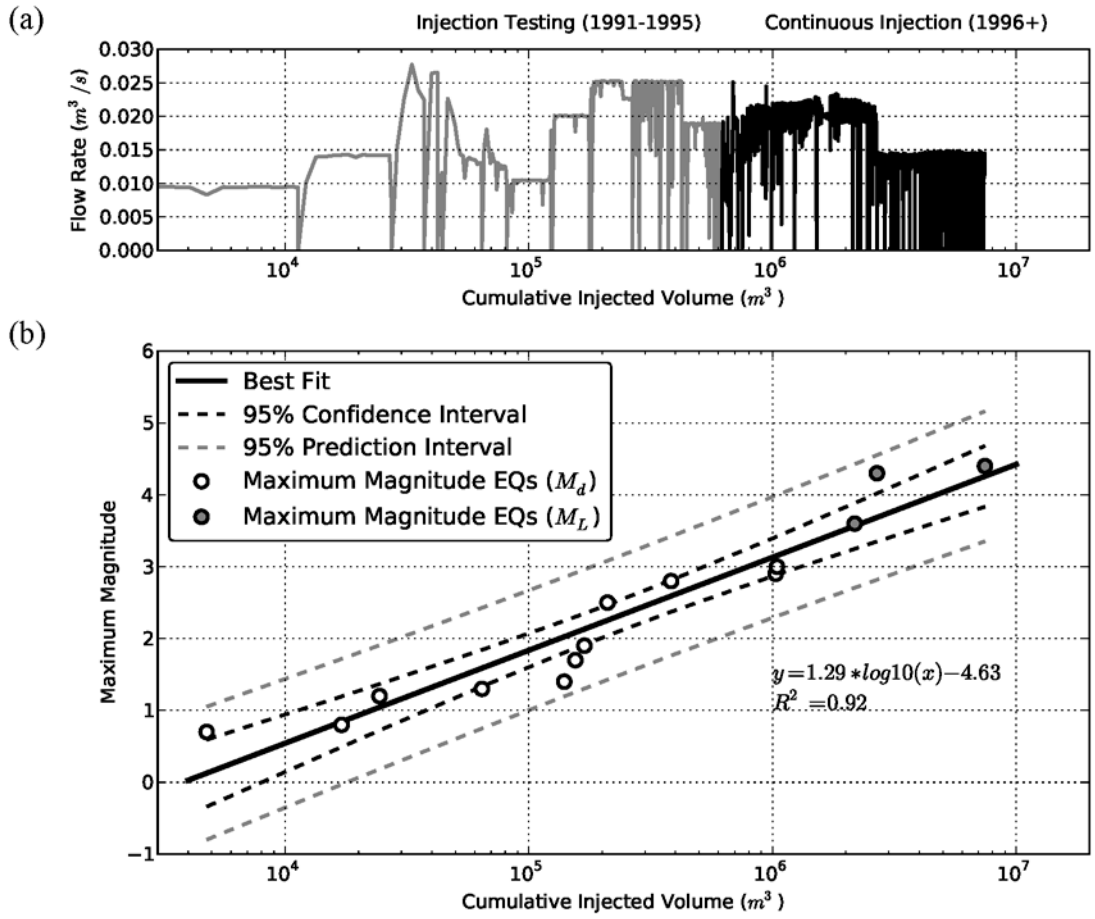

Figure 21 - From Yeck at el. (2015). (a) Flow rate as a function of the cumulative injected volume. The gray line shows the flow rate during the injection tests (1991 - 1995), while the black line shows the flow rates during long-term injection (1996 – 2013). (b) Observed maximum magnitude PVU-induced earthquakes as a function of the cumulative injected volume. Least squares fit shown in black, with 95% confidence interval (black dashed) and 95% prediction interval (gray dashed).

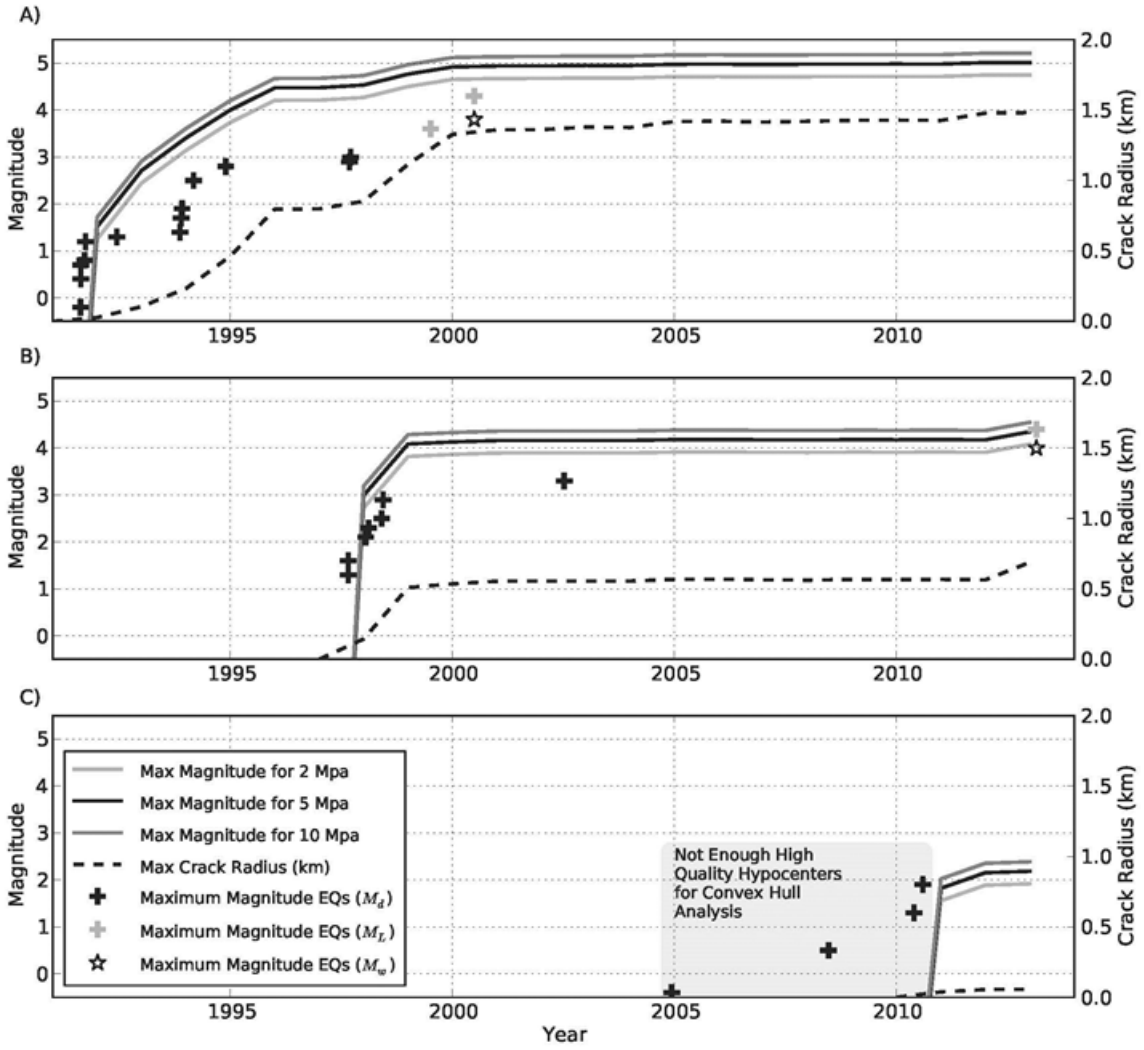

Figure 22 - From Yeck at el. (2015). Maximum crack radius and maximum earthquake magnitude as a function of time for the A) Nearwell, B) Northwest, and C) Southeast clusters. Observed maximum magnitudes through time are shown as crosses and stars.

5 Conclusions

The current MASIP, 5350 psi, was selected based on a calculated 6106 psi surface injection pressure threshold necessary to fracture the confining salt layer. Since the time of these initial calculations, little subsequent analysis has been performed in regards to the confining ability of the Paradox Salt formation. Therefore, with the analyses performed to date, 6106 psi remains the best estimate for the surface injection pressure necessary to fracture the salt. The uncertainty in this calculated limit is unknown and may warrant further investigation. In addition, the subsurface has been altered since the initiation of injection at the PVU, and potential effects of changing subsurface conditions on the confining ability of the salt have not been evaluated.

Increasing average wellhead pressures in response to an increase in the MASIP would likely lead to adverse changes in the seismicity induced by injection. Based on patterns observed to date, an increase in average surface injection pressures would likely lead to increased seismicity rates and likelihood of felt events ($M \geq 2.5$), at least in the near-well area. Increased pressures could cause seismicity to spread to regions that were previously aseismic, as was observed in 2009-2012 when wellhead pressures were high. Sustained increased injection pressures could potentially cause pore pressures to increase sufficiently to cause seismicity clusters to grow and thereby increase maximum earthquake magnitude within the clusters. Seismicity clusters which are currently small (and to date have only experienced events with small magnitude) may be the most susceptible to these effects.

6 References

Block, L., and Wood, C., 2009, *Overview of PVU-Induced Seismicity from 1996 to 2009 and Implications for Future Injection Operations*, Technical Memorandum No. 86-68330-2009-22, Bureau of Reclamation, Denver, Colorado, pp. 13.

Block, L., and Wood, C., 2011, *2010 Annual Report, Paradox Valley Seismic Network, Paradox Valley Project, Colorado*, Technical Memorandum No. 86-68330-2011-16, Bureau of Reclamation, Denver, Colorado, pp. 77.

Block, L., and Wood, C., 2012, *2011 Annual Report, Paradox Valley Seismic Network, Paradox Valley Project, Colorado*, Technical Memorandum No. 86-68330-2012-16, Bureau of Reclamation, Denver, Colorado, pp. 60.

Block, L. Yeck, W., King, V., Derouin, S., and Wood., C., 2012, *Review of Geologic Investigations and Injection Well Site Selection, Paradox Valley Unit, Colorado*, Technical Memorandum No. 86-68330-2012-27, Bureau of Reclamation, Denver, Colorado, pp. 71.

Block, L., and Wood, C., 2013, *2012 Annual Report, Paradox Valley Seismic Network, Paradox Valley Unit, Colorado*, Technical Memorandum No. 86-68330-2013-23, Bureau of Reclamation, Denver, Colorado, pp. 54.

Block, L.V., Wood, C.K., Yeck, W.L. and King, V.M., 2014, The 24 January 2013 M_L 4.4 Earthquake near Paradox, Colorado, and Its Relation to Deep Well Injection, Seismological Research Letters, 85, 609-624.

Block, L., Meremonte, M., Yeck, W., King, V., Besana-Ostman, G., and Wood, C., 2015a, *2014 Annual Report, Paradox Valley Seismic Network, Paradox Valley Unit, Colorado*, Technical Memorandum No. 85-833000-2015-07, Bureau of Reclamation, Denver, Colorado, pp. 90.

Block, L.V., Wood, C.K., Yeck, W.L. and King, V.M., 2015b, Induced seismicity constraints on subsurface geological structure, Paradox Valley, Colorado, Geophysical Journal International, 200, 1172-1195

Bremkamp, W. and Harr, C.L., 1988, *Area of Least Resistance to Fluid Movement and Pressure Rise, Paradox Valley Unit Salt Brine Injection Project, Bedrock, Colorado*, Report to the Bureau of Reclamation, pp. 39.

Bremkamp, W., Harr, C.L. and Prather, O.E., 1984, *Geophysical interpretation - Seismic data, Paradox Valley Unit, Montrose County, Colorado*, Report 3-CS-40-0146B to Bureau of Reclamation, pp. 24.

Bureau of Reclamation, 1997. *Paradox Valley Unit Final Supplemental Definite Plan Report and Environmental Assessment*, pp. 189.

Campbell, J.A., 1981, Summary of Paleozoic stratigraphy and history of western Colorado and eastern Utah, in *Western Slope Colorado: New Mexico Geological Society 32nd Field Conference Guidebook*, pp. 81-87.

Dewan, J.T., 1987a, Letter to Ken E. Davis Associates (January 15, 1987), Re: BOR Paradox Valley Injection Test Well #1, Logs run in the surface hole (2012-90 ft), Dewan and Timko Inc., Houston, pp. 6.

Dewan, J.T., 1987b, Letter to Ken E. Davis Associates (June 22, 1987), Re: BOR Paradox Valley Injection Test Well #1, Logging of the Intermediate Hole (14,050 to 2,020 ft) of BOR Paradox Valley Injection Test Well #1, Dewan and Timko Inc., Houston, pp. 8.

Dewan, J.T., 1987c, Letter to Ken E. Davis Associates (August 20, 1987), Re: BOR Paradox Valley Injection Test Well #1, Logging of the Liner Hole (15,950 to 14,050 ft) of BOR Paradox Valley Injection Test Well #1, Dewan and Timko Inc., Houston, pp. 7.

Dewan, J.T., 1988a, Letter to Ken E. Davis Associates, Re: BOR Paradox Valley Injection Test Well #1 (January 27, 1988), Summary of Log Interpretation for BOR Paradox Valley Injection Test Well #1 14,050 to 15,950 ft Interval, Dewan and Timco, Inc., Houston, pp. 32.

Dewan, J.T., 1988b, Letter to John J. Brown, Bureau of Reclamation, Re: BOR Paradox Valley Injection Test Well #1 (January 28, 1988), Listing of open-hole logs generated for Fenix and Scisson, BOR Paradox Valley Injection Test Well No. 1, Dewan and Timko, Inc., Houston, pp. 3.

Dewan, J.T., 1988c, Letter to Jim Bundy, Re: BOR Paradox Valley Injection Test Well #1 (July 20, 1998), Dewan and Timco, Inc., Houston, pp. 2.

Dewan, J.T., 1988d, Letter to Jim Bundy, Re: BOR Paradox Valley Injection Test Well #1 (September 21, 1998), Dewan and Timco, Inc., Houston, pp. 2.

Doelling, H., 1988, Geology of Salt Valley anticline and Arches National Park, Grand County, Utah, in *Salt Deformation in the Paradox Region*, Utah Geological and Mineral Survey Bulletin 122, 1-60.

Envirocorp Services and Technology Inc., 1995, *Report of Evaluation of Injection Testing for Paradox Valley Injection Test No. 1*, Report to Bureau of Reclamation, Durango, CO, pp. 67.

Environmental Protection Agency, 1997, Fact Sheet: Application of Reauthorization of an Underground Injection Control Permit for a Class V Well, pp. 46.

Environmental Protection Agency, 2004, Final addendum to the statement of basis for an Environmental Protection Agency (EPA) major permit modification no. 3 to the United States Bureau of Reclamation (USBR) class V brine disposal well final permit: CO50108-00647; Paradox Salinity Control Well No. 1, Montrose County, Colorado, pp. 15.

Environmental Protection Agency, 2011, Underground Injection Control Program Permit for Reauthorization, pp. 90.

Gutiérrez, F., 2004, Origin of the salt valleys in the Canyonlands section of the Colorado Plateau: Evaporite-dissolution collapse versus tectonic subsidence, Geomorphology, 57, 423-435.

Harr, C.L., 1988, *Final Geological Well Report, Bureau of Reclamation Injection Test Well No. 1, Paradox Valley, Montrose County, Colorado,* Grand Junction, Colorado, pp. 141.

Huntoon, P., 1988, Late Cenozoic gravity tectonic deformation related to the Paradox salts in the Canyonlands area of Utah, in *Salt Deformation in the Paradox Region*, Utah Geological and Mineral Survey Bulletin 122, 81-93.

Katz, L.J. and Carroll, R., 1984, *Geophysical Interpretation of Seismic Data, Paradox Valley Unit*, Report to Bureau of Reclamation, Utah Geophysical, Inc., pp. 31.

King, V.M. and Block, L. (2015), *Evidence for Far-field Reservoir Pressurization, Paradox Valley, Colorado* (Draft), Technical Memorandum No. 85-833000-2014-42, Bureau of Reclamation, Denver, Colorado.

King, V.M., Block, L.V., Yeck, W.L., Wood, C.K. and Derouin, S.A., 2014, Geological structure of the Paradox Valley Region, Colorado, and relationship to seismicity induced by deep well injection, Journal of Geophysical Research: Solid Earth, 119, 4955–4978.

Kraaijpoel, D., and Dost, B., 2013, Implications of salt-related propagation and mode conversion effects on the analysis of induced seismicity. Journal of Seismology, 17, 95-107.

McClure, K., Morgan, C.D., Chidsey, T.C. Jr., Eby, D.E., and Scott,P., 2003, *Utah and Colorado: Targets for increased oil production and reserves using horizontal drilling techniques*: Utah Geologic Survey Contract No. DE-2600BC15128, Deliverable 1.1.2 Regional Paradox Formation Cross Sections, Blanding sub-basin, Utah and Colorado, pp. 29.

Nuccio, V.F. and Condon, S.M., 1996, Burial and thermal history of the Paradox Basin, Utah and Colorado, and petroleum potential of the middle Pennsylvanian Paradox Formation, in *Evolution of Sedimentary Basins – Paradox Basin*, A. C. Huffman Jr., Project Coordinator, U. S. Geological Survey Bulletin 2000-O, pp. 47.

Suburface Technology, 2001, *Report of Operations*, Report to United States Department of the Interior, Bureau of Reclamation, Montrose County, Colorado, Subsurface Technology Inc. Project No. 60D5207, Houston, pp. 24.

Walker, J.D., Geismman, J.G. and (Compilers), 2009, Geologic Time Scale, Geological Society of America.

Wang, H., Detournay, E., Dusseault, M., Fehler, M., and Frohlich, C., 2015, *Report from the Consultant Review Board on Paradox Valley Unit- MASIP/Induced Seismicity Meeting No. 1, January 28-31, 2015, Grand Junction, Colorado*, pp 35.

Williams, P.L., 1964, Geology, structure, and uranium deposits of the Moab quadrangle, Colorado and Utah, U.S. Geological Survey map.

Wood C.K., Block L.V., King V.M, and Yeck, W.L. (2015), *The M_L 4.4 Earthquake of January 24, 2013, Near Paradox, Colorado, and Implications for Near-term Injection Operations* (Draft), Technical Memorandum No. 86-68330-2013-12, Bureau of Reclamation, Denver, Colorado.

Yeck, W.L., Block, L.V., Wood, C.K. and King, V.M., 2015, Maximum magnitude estimations of induced earthquakes at Paradox Valley, Colorado, from cumulative injection volume and geometry of seismicity clusters, Geophysical Journal International, 200, 322-336.